Post-Test Examination of the WWER Bundle QUENCH-12

G. Schanz[3], U. Stegmaier[1], M. Heck[3], J. Stuckert[3]
Institut für Materialforschung ([3]IMF III, [1]IMF I)

presented by G. Schanz

13th International QUENCH Workshop, Forschungszentrum Karlsruhe, November 20-22, 2007

Contents

- **Reminder of QUENCH-12 test conduct and data acquisition**
- **Post-test examination at FZK, qualitative results**
- **FZK data on the bundle oxidation extent**
- **Conclusive summary**

WWER bundle QUENCH-12 cross section, top view

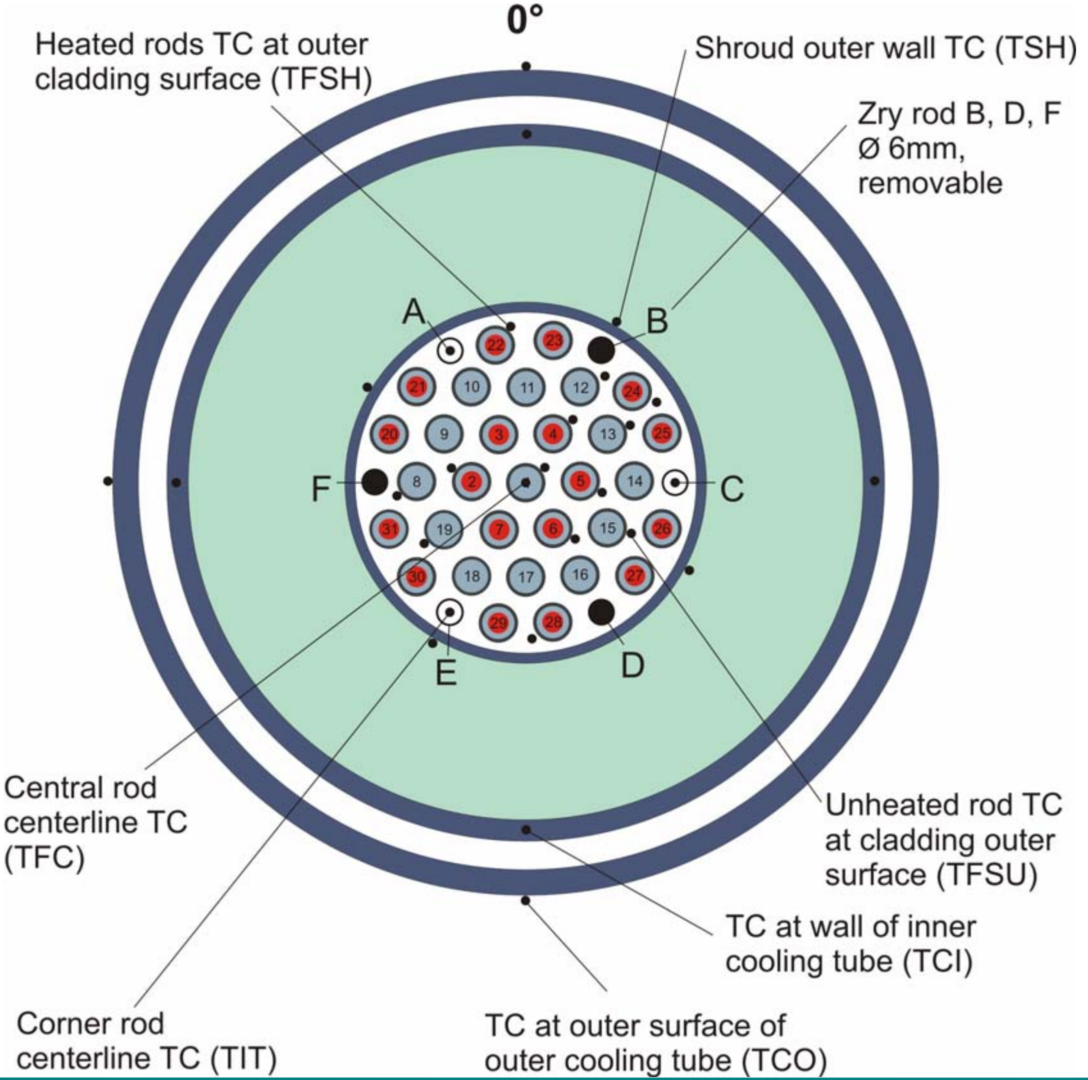

Comparison of power and temperature profiles for QUENCH-12 and QUENCH-06

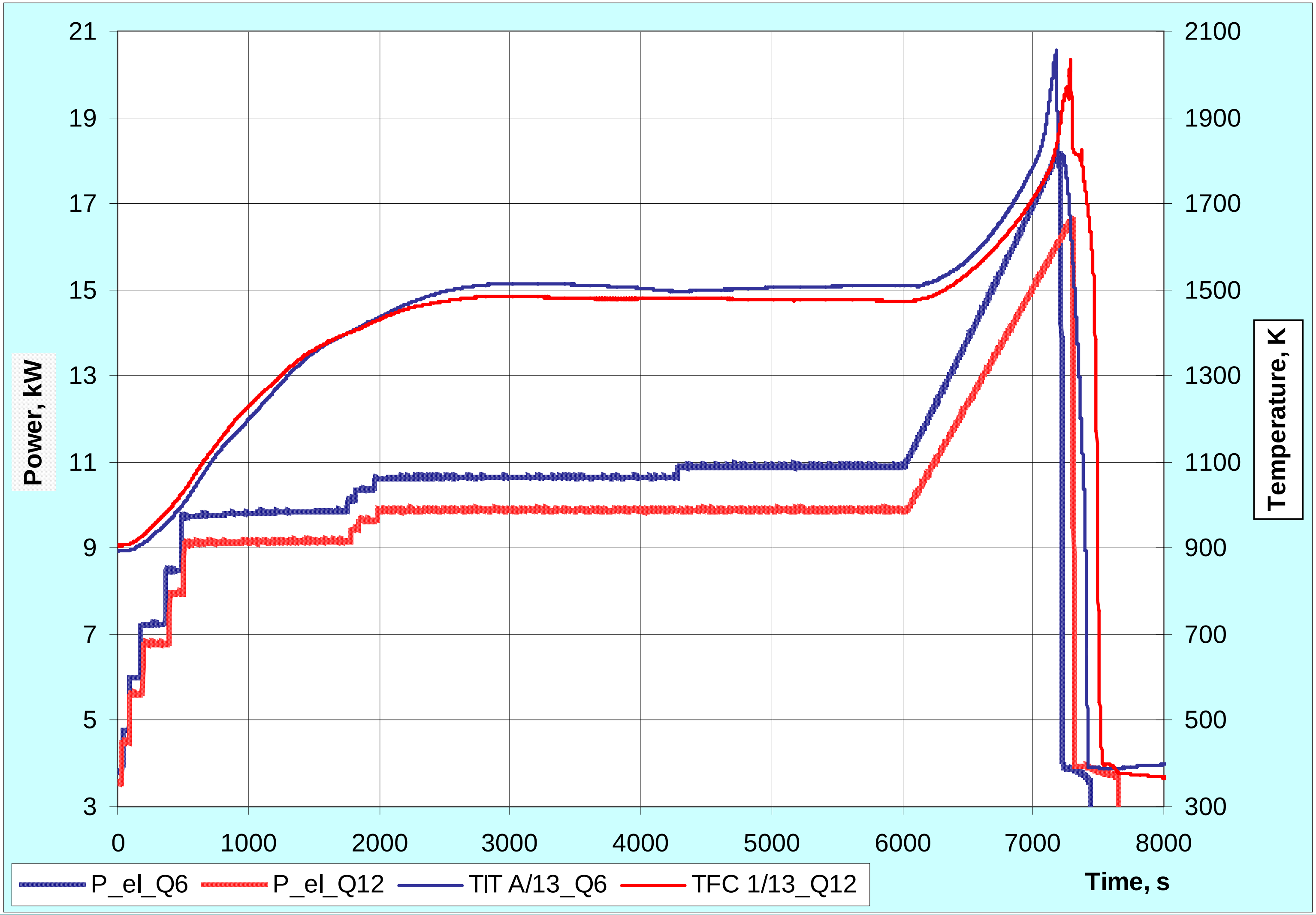

QUENCH-12, quench phase: selected reading of the bundle thermocouples. Quench front propagation. Cooling of the bundle during ~350 s

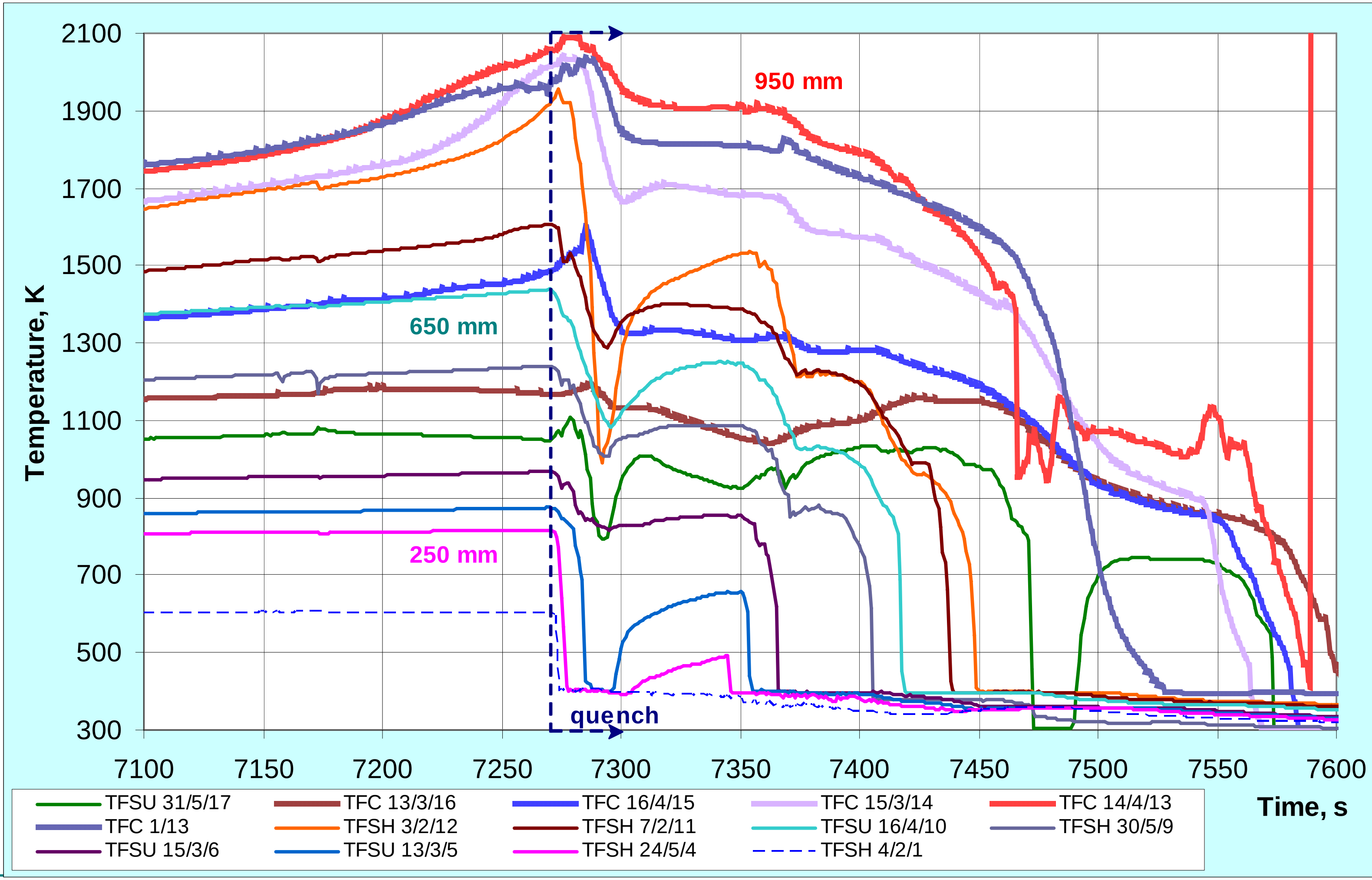

Comparison of hydrogen release during QUENCH-12 and QUENCH-06

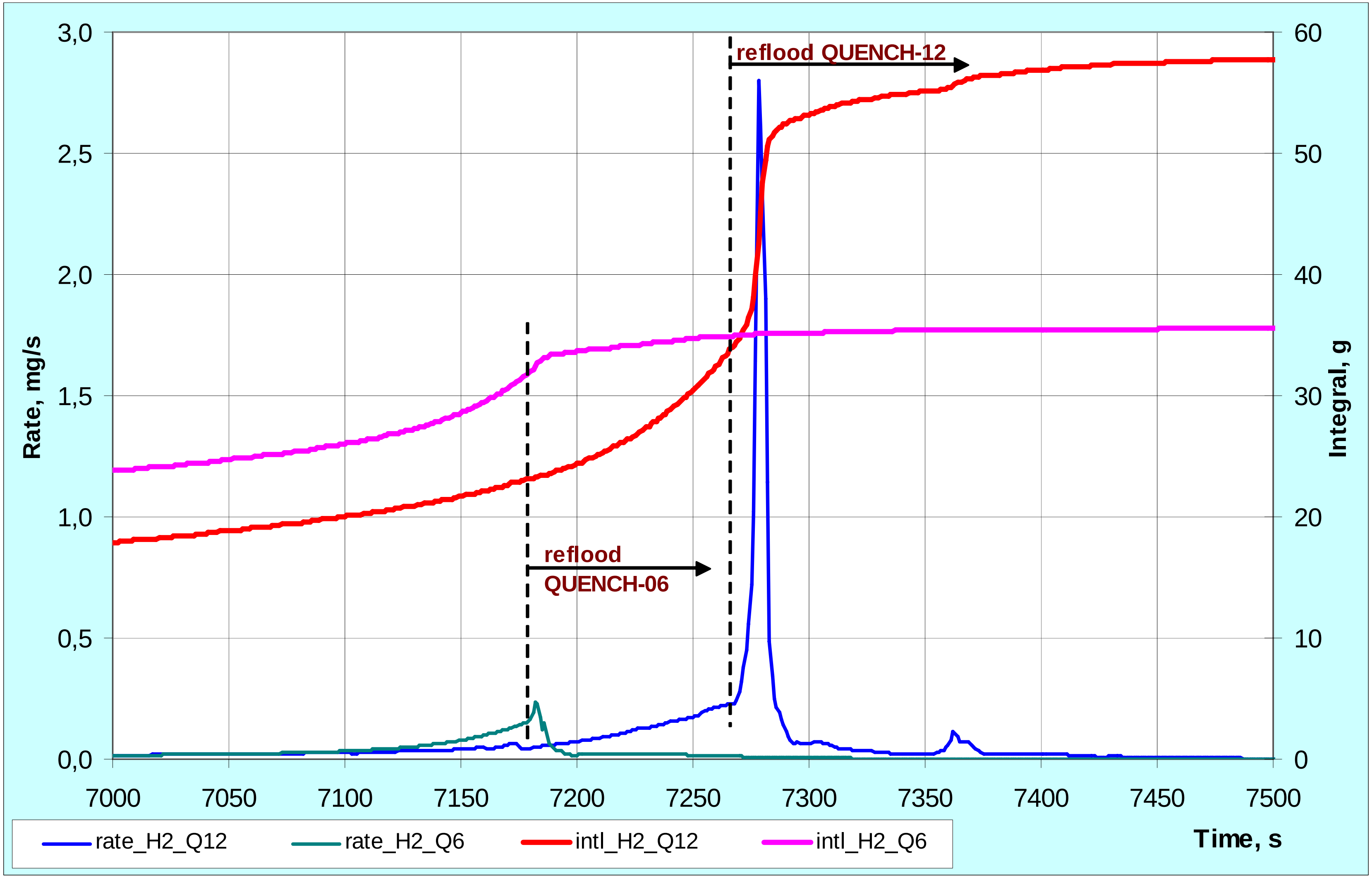

QUENCH-12; cross section overview at 550 mm elevation

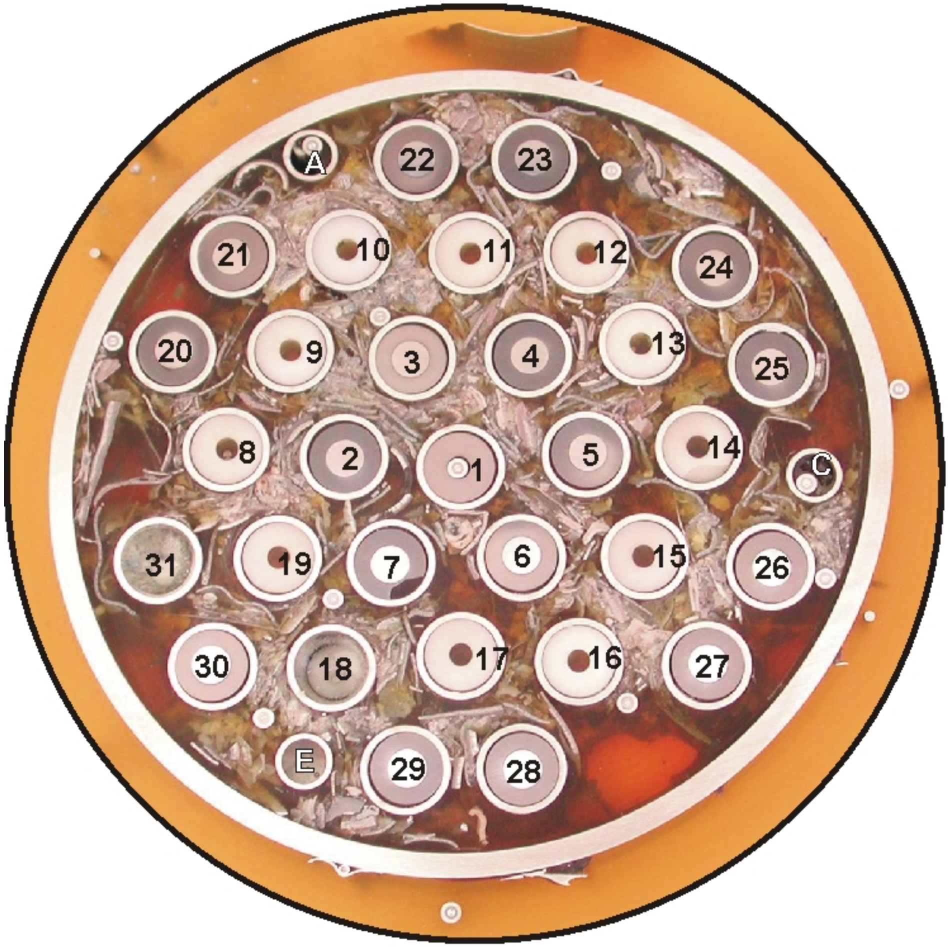

Elevation 550mm, top view

Elevation 534 mm, inverted to top view

QUENCH-12, level 550 mm; oxidation of the central rod

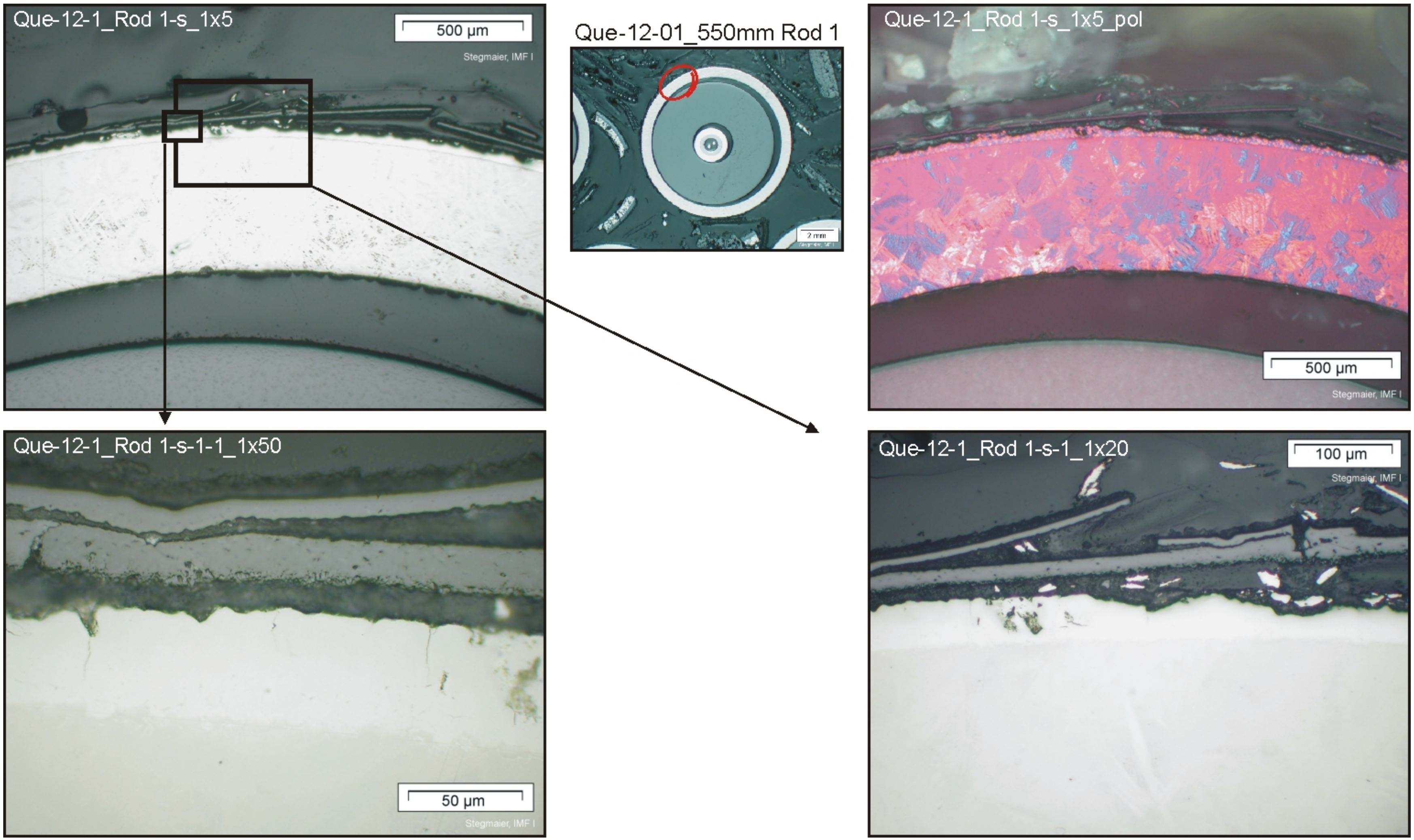

QUENCH-12, level 550 mm; oxidation of rod 5

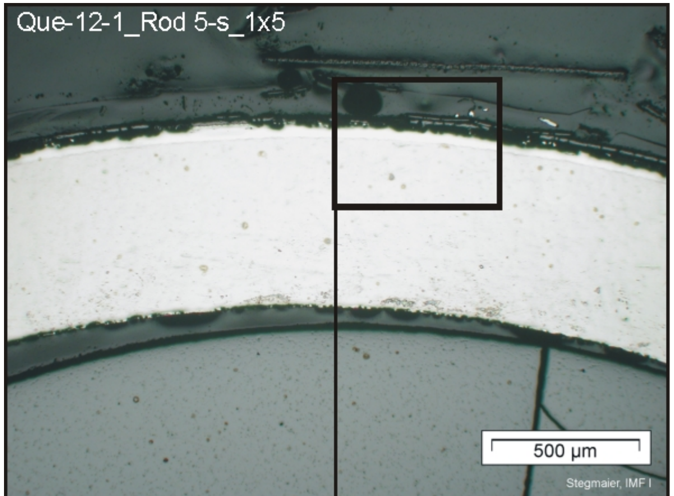

Que-12-01_550mm Rod 5

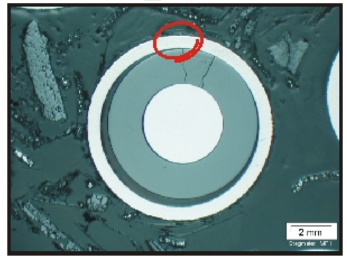

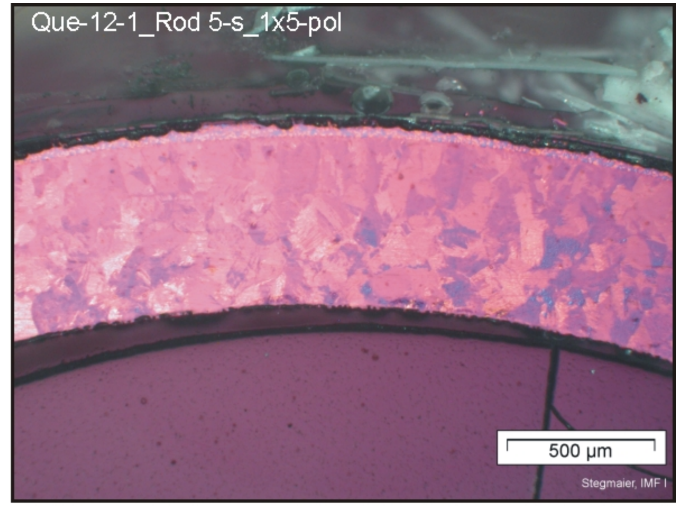

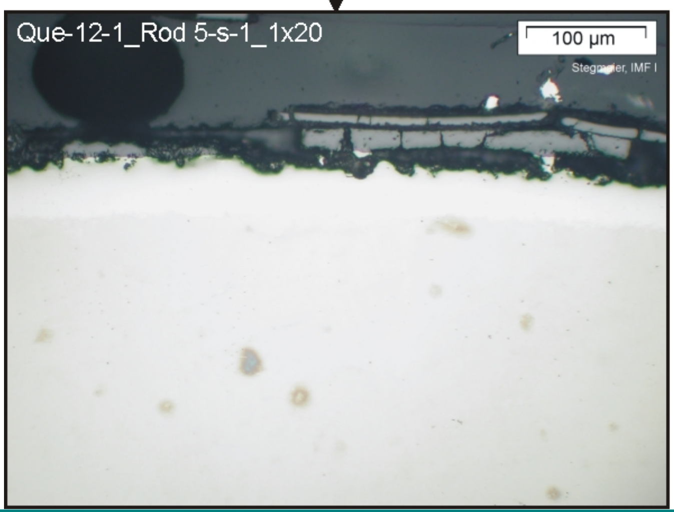

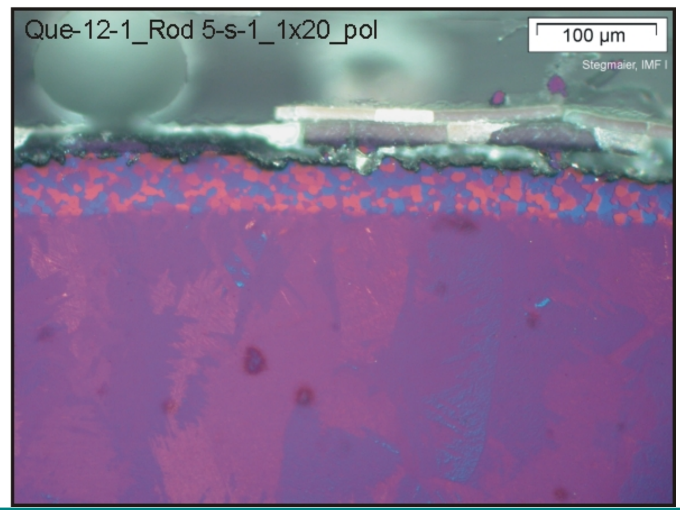

QUENCH-12, level 550 mm; cladding debris showing both-sided oxidation

Debris fragments between two rods

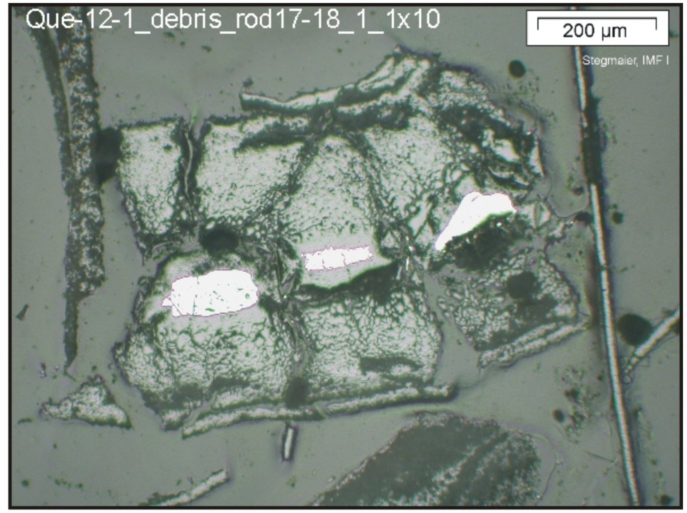

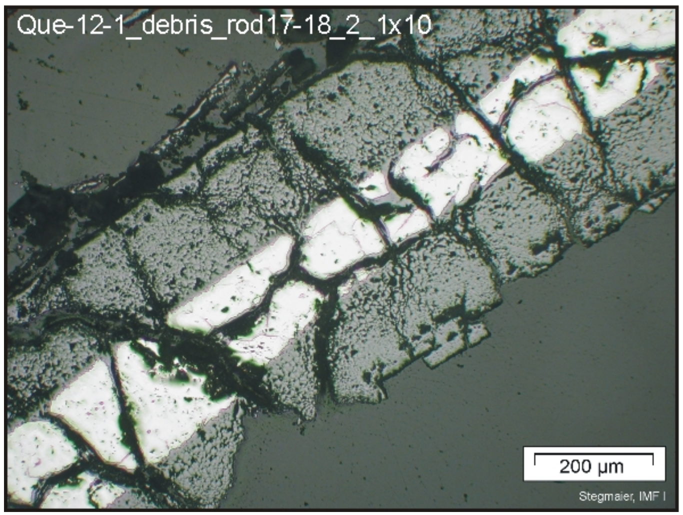

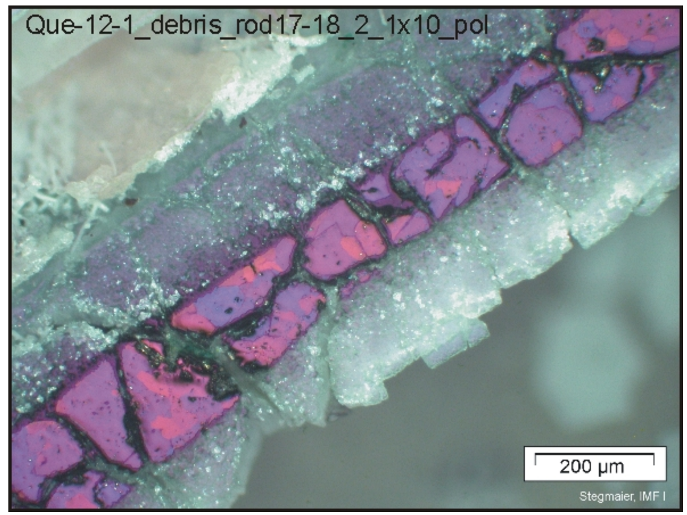

QUENCH-12; cross section overview at 650 mm elevation

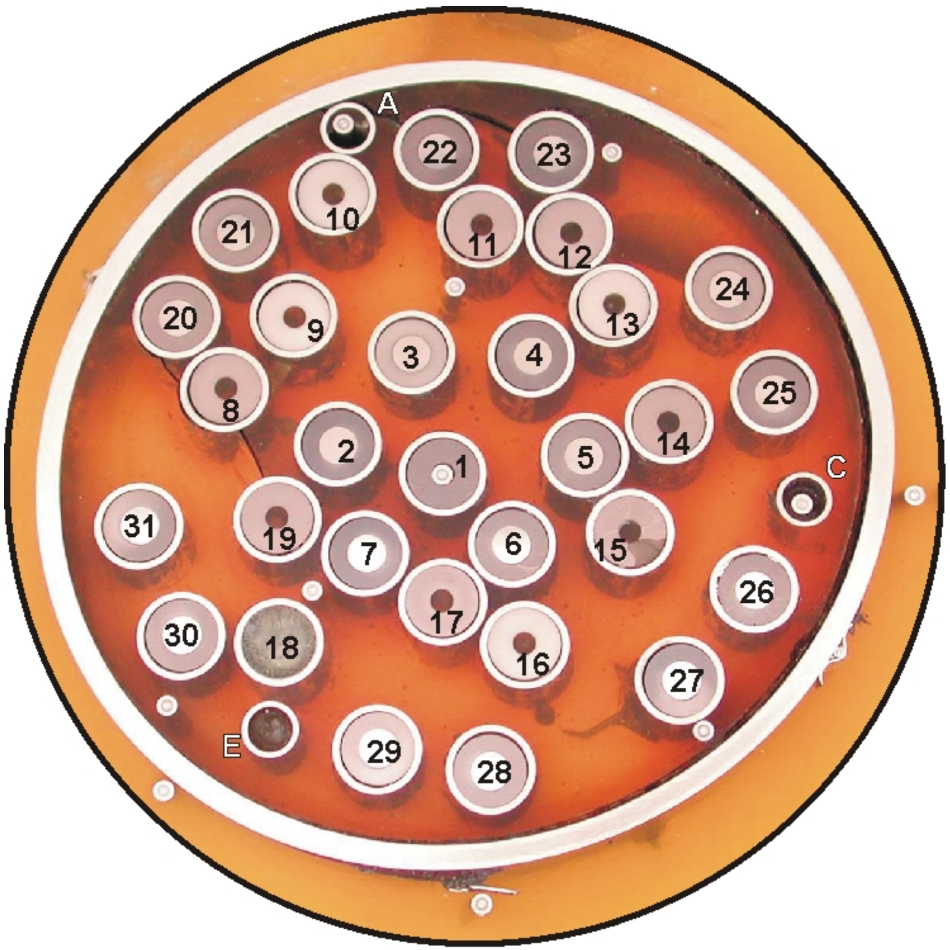

Elevation 650mm, top view

Elevation 634 mm, inverted to top view

QUENCH-12, level 650 mm; oxidation of the central rod

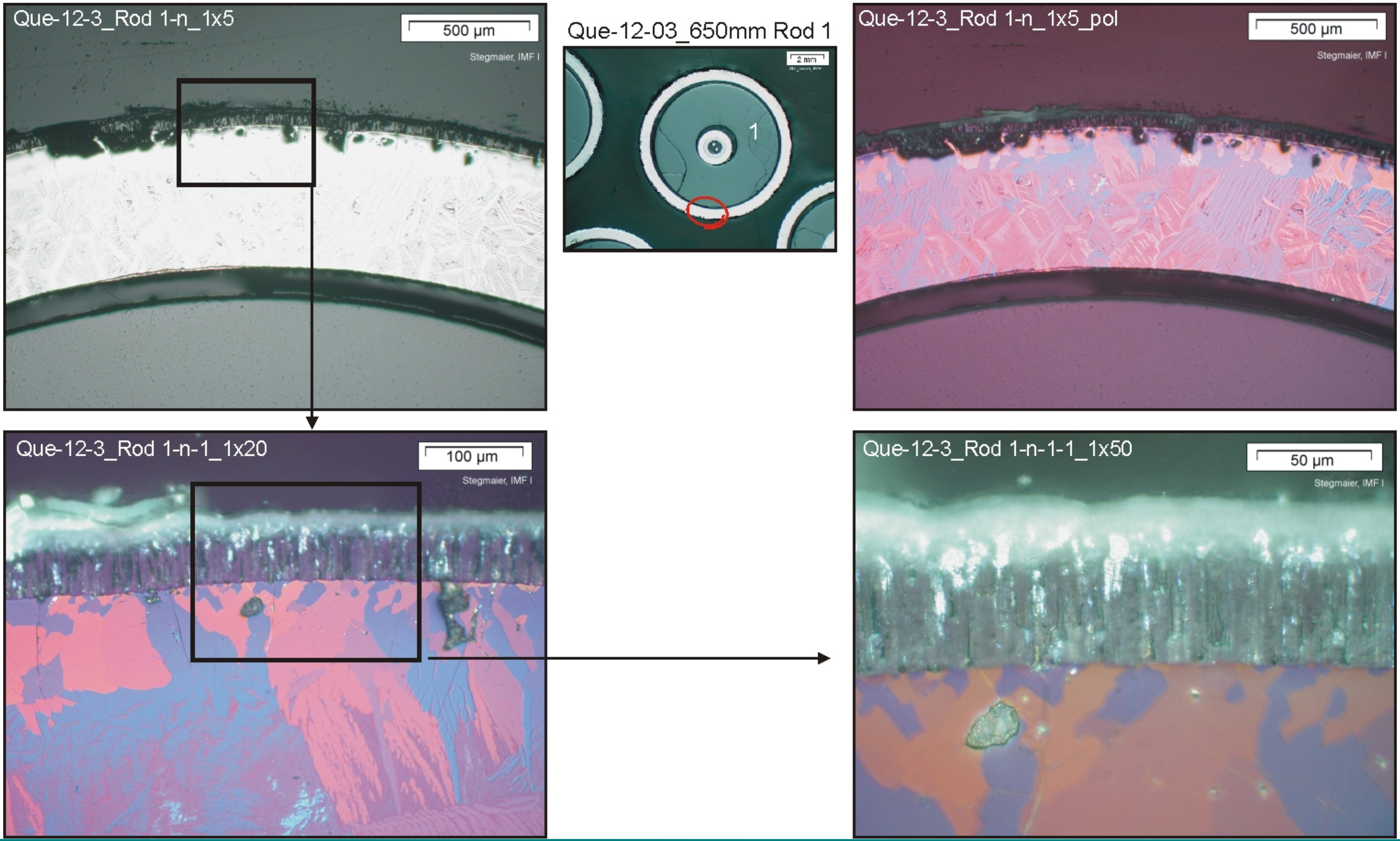

QUENCH-12, level 650 mm; oxidation of rods 4 (left) and 18 (right)

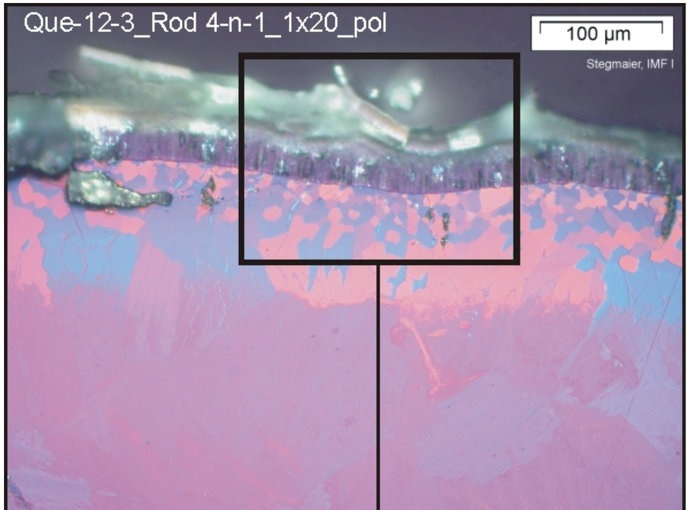

Que-12-03_650mm Rod 4

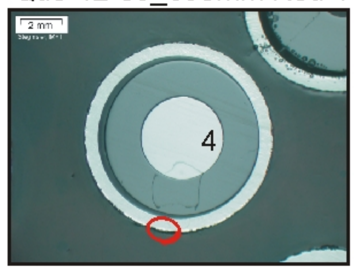

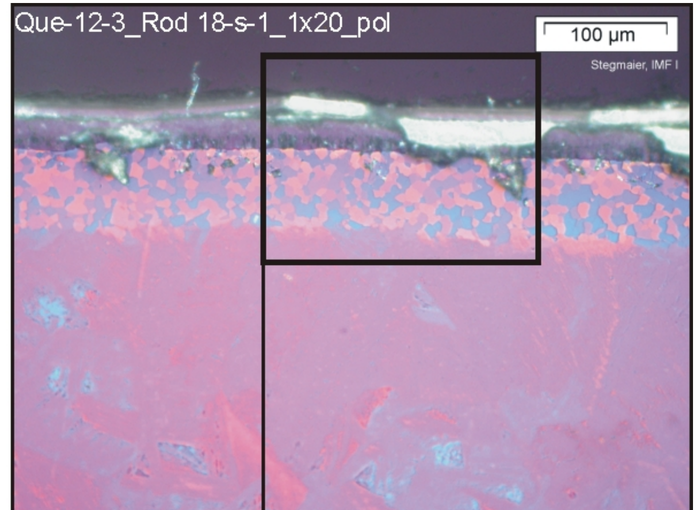

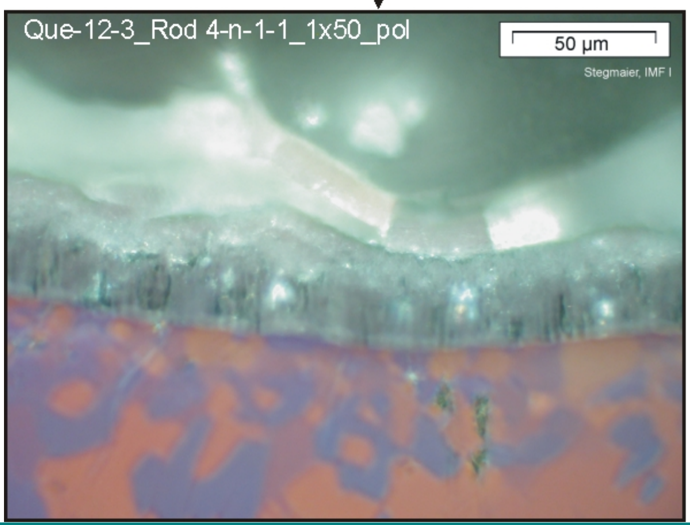

Que-12-03_650mm Rod 18

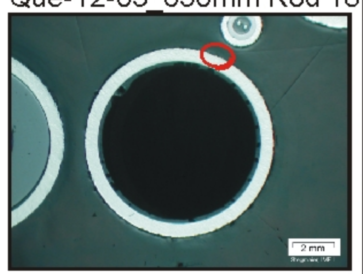

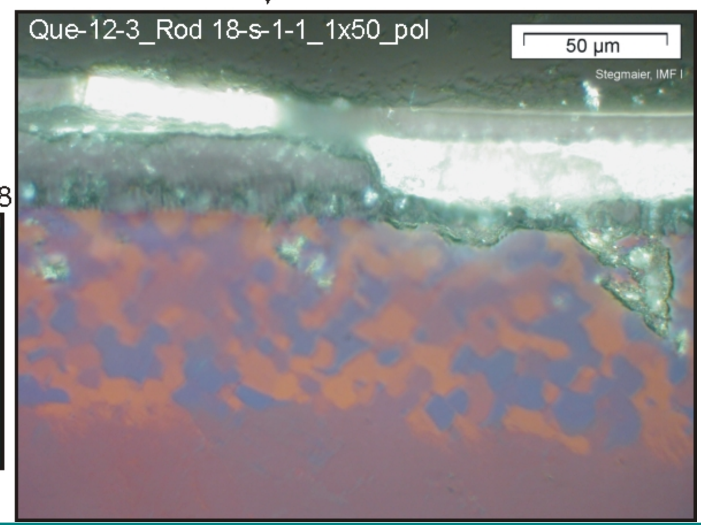

QUENCH-12; cross section overview at 750 mm elevation

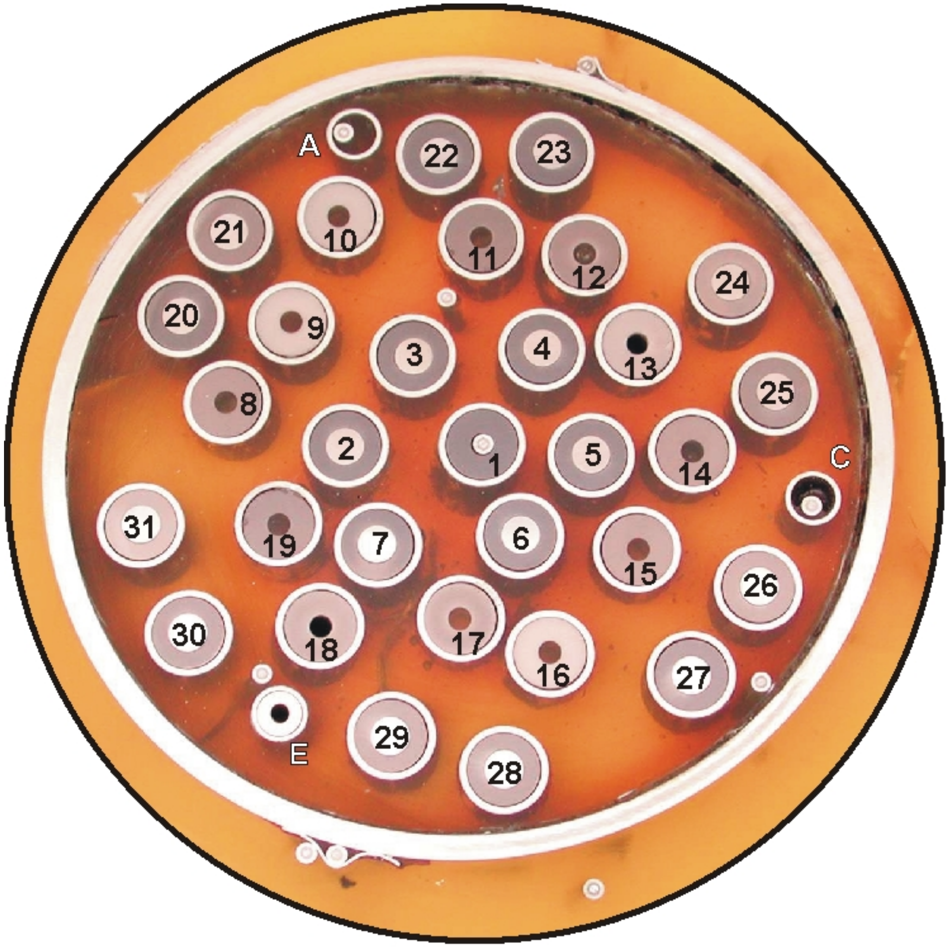

Elevation 750mm, top view

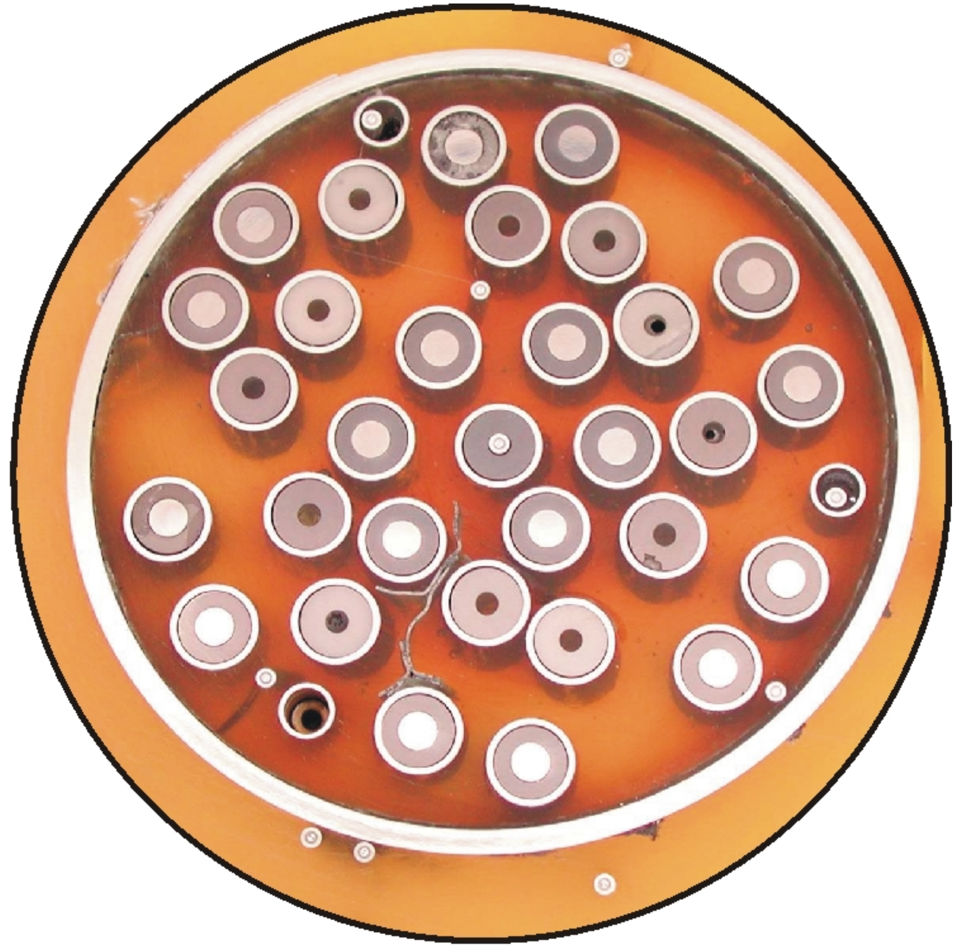

Elevation 734 mm, inverted to top view

QUENCH-12, level 750 mm; oxidation of central rod (top) and rod 2 (bottom)

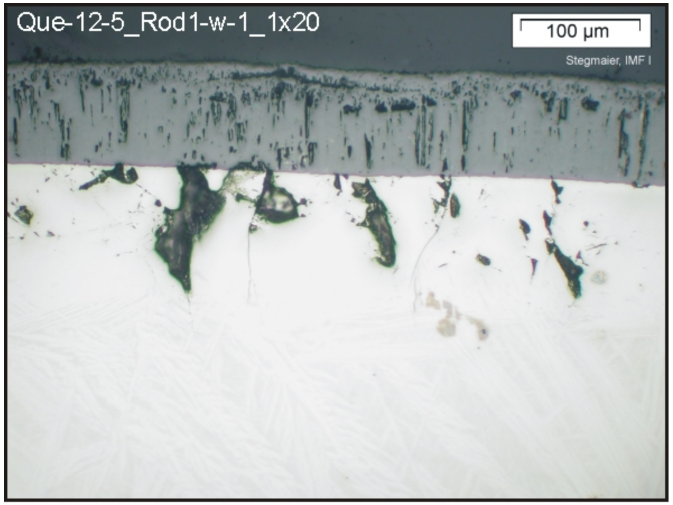

Que-12-05_750mm Rod 1

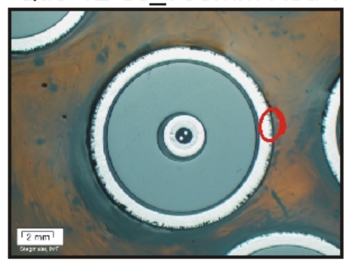

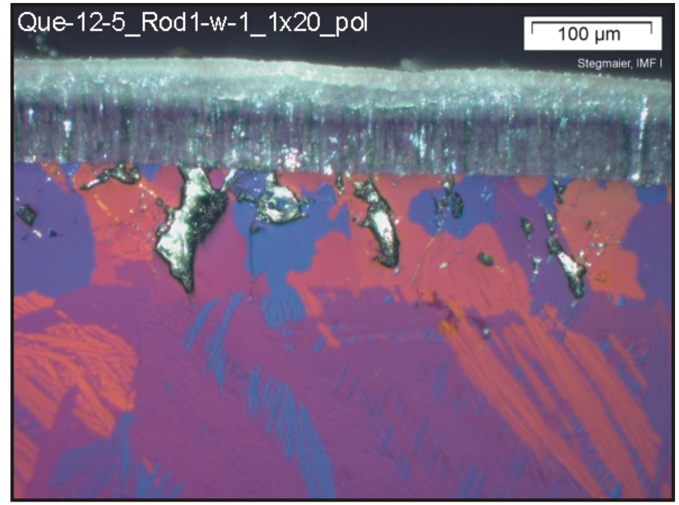

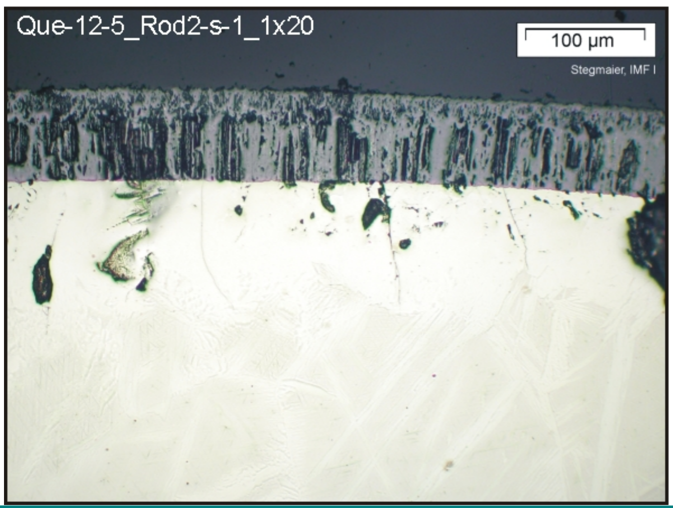

Que-12-05_750mm Rod 2

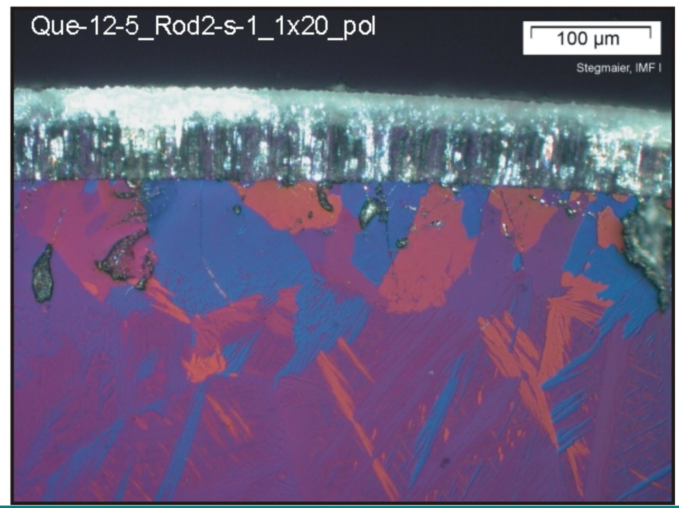

QUENCH-12, level 750 mm; oxidation of rod 17 (top) and 24 (bottom)

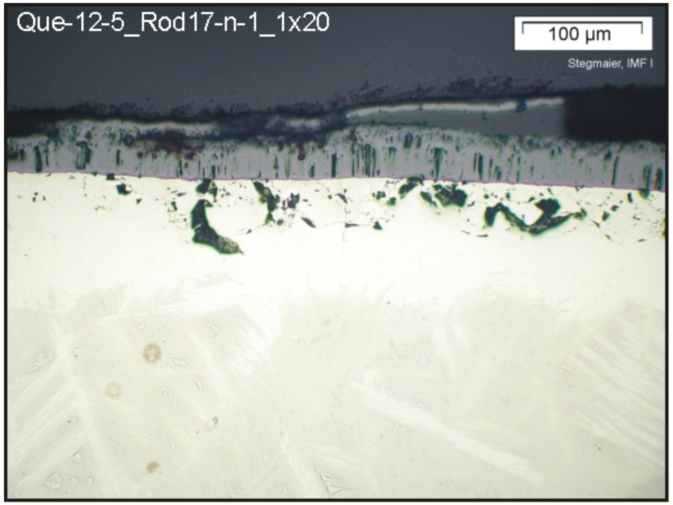

Que-12-07_750mm Rod 17

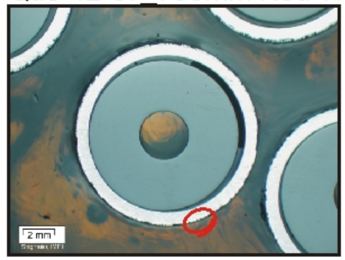

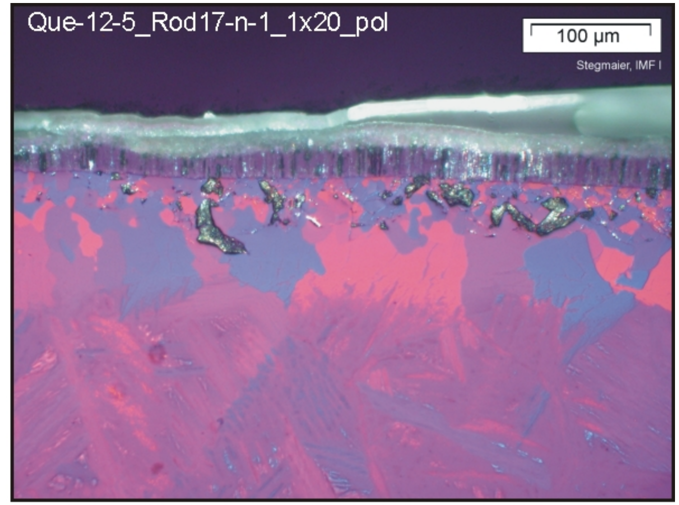

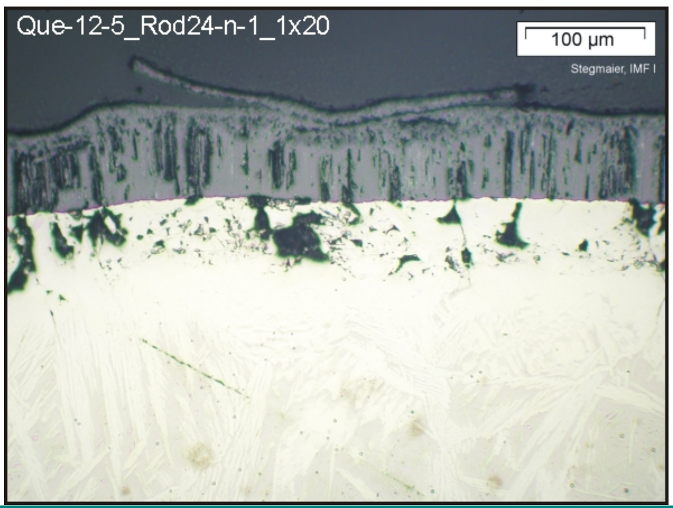

Que-12-5_750mm Rod 24

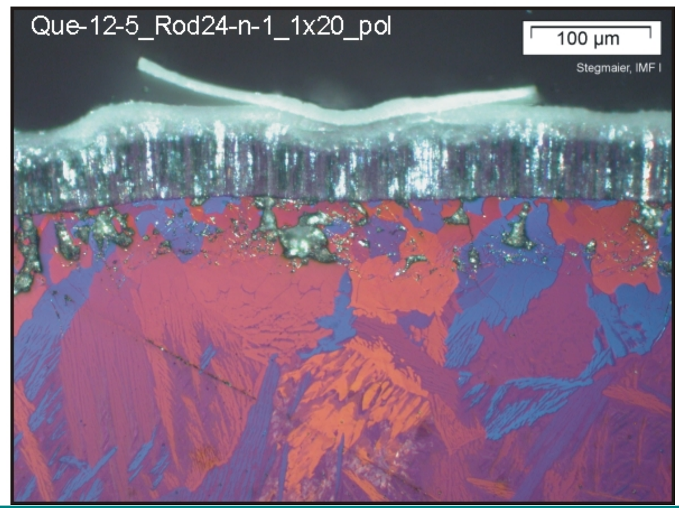

QUENCH-12; cross section overview at 850 mm elevation

Elevation 850mm, top view

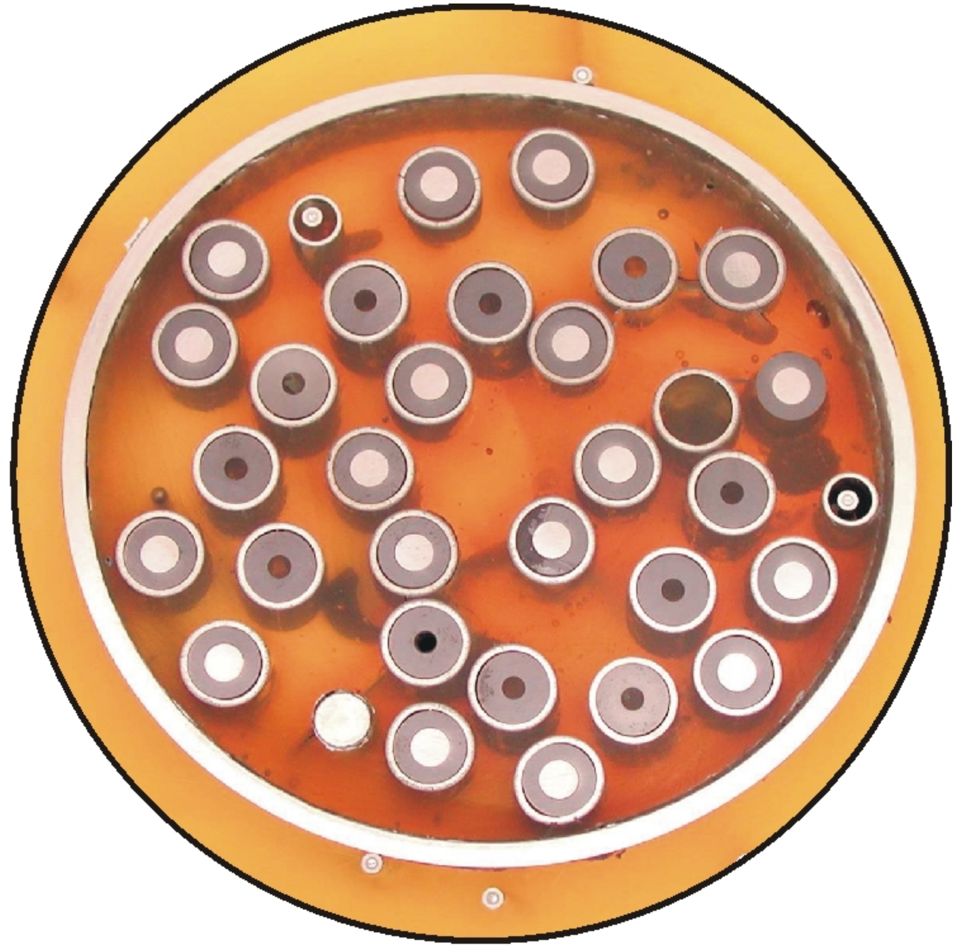

Elevation 834 mm, inverted to top view

QUENCH-12, level 850 mm; special items of the oxidation extent of rods

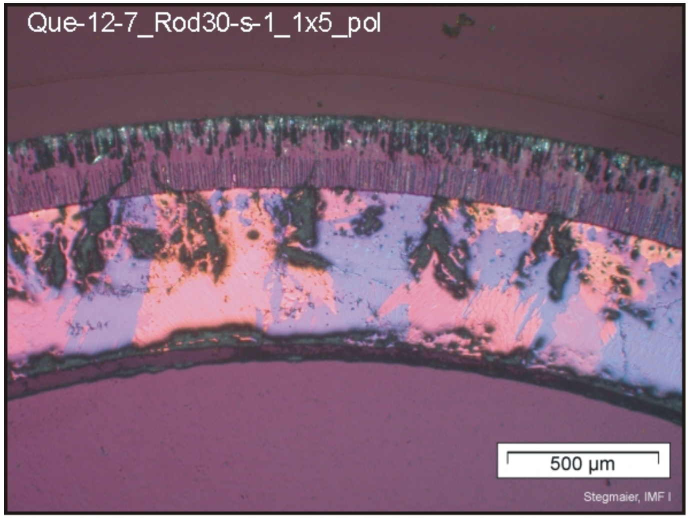

Rod 30; cladding matrix converted to α-Zr(O) phase

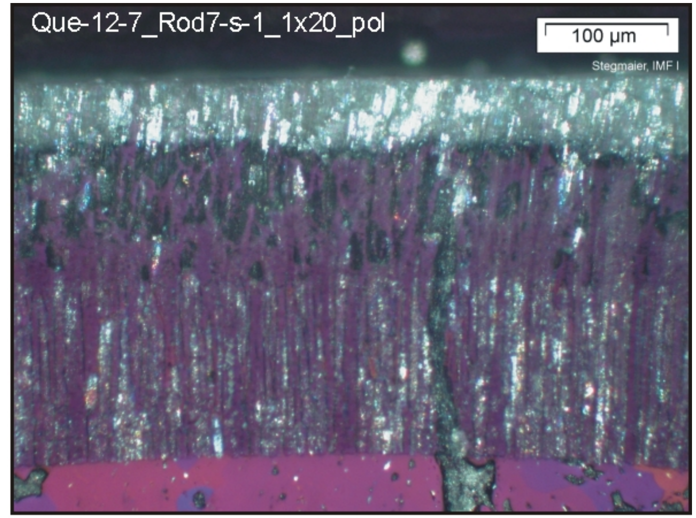

Rod 7; ZrO_2 scale composed of top layer(s), columnar tetragonal phase oxide, prior cubic phase oxide; metallic cladding substrate mostly α-Zr(O) phase

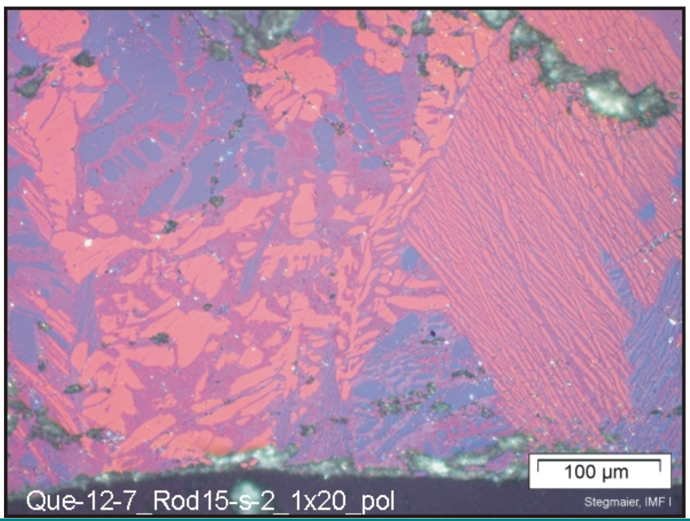

Rod 15; cladding matrix at inner rim retained as β-Zr phase

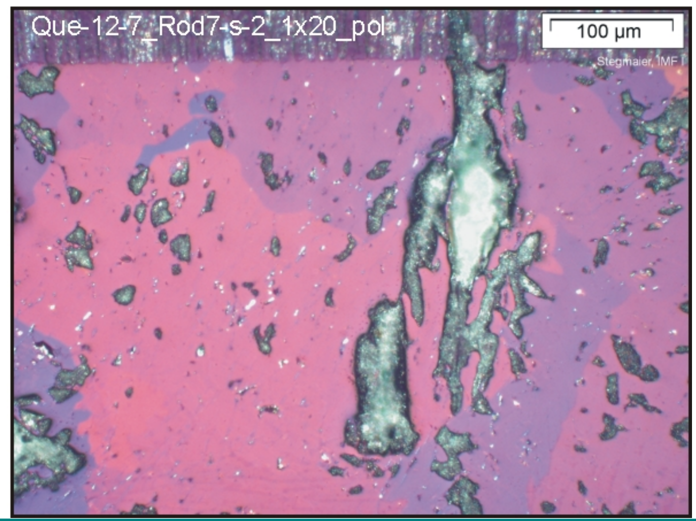

QUENCH-12, level 850 mm; small melt pool in contact to rod 25

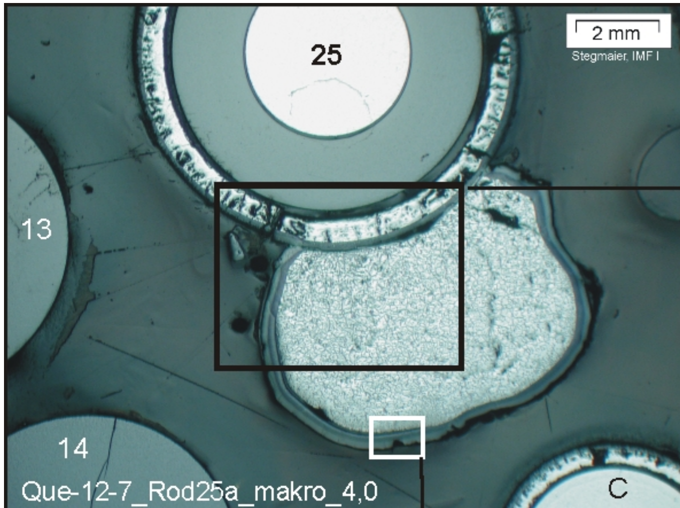

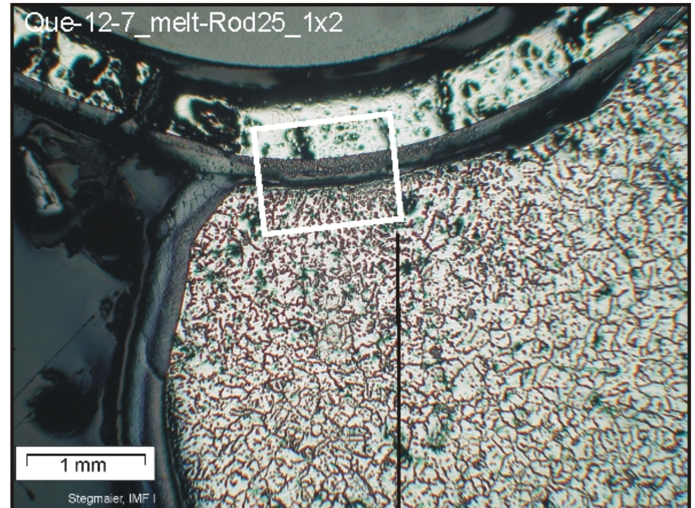

The melt-embedded scale of rod 25 shows a tendency to internal dissolution

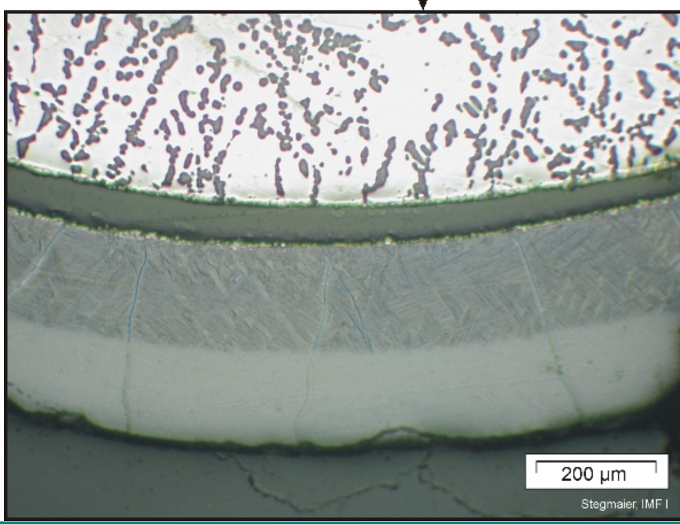

Thick melt pool scale indicates a strong melt oxidation

Duplex phase $Zr(O)/ZrO_2$ melt microstructure

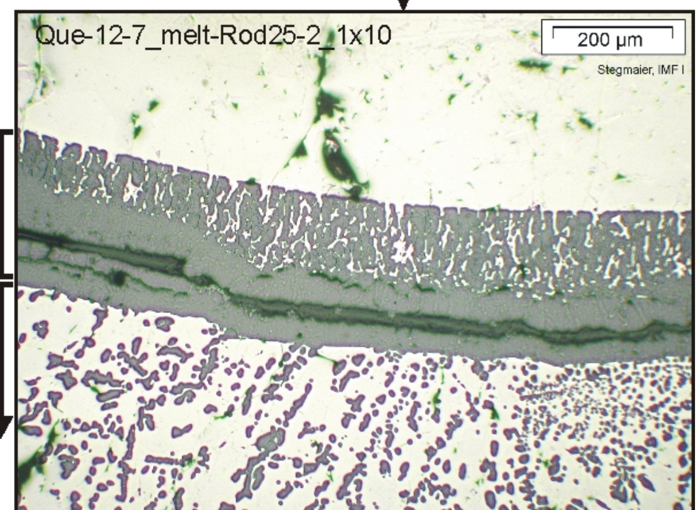

QUENCH-12; cross section overview at 950 mm elevation

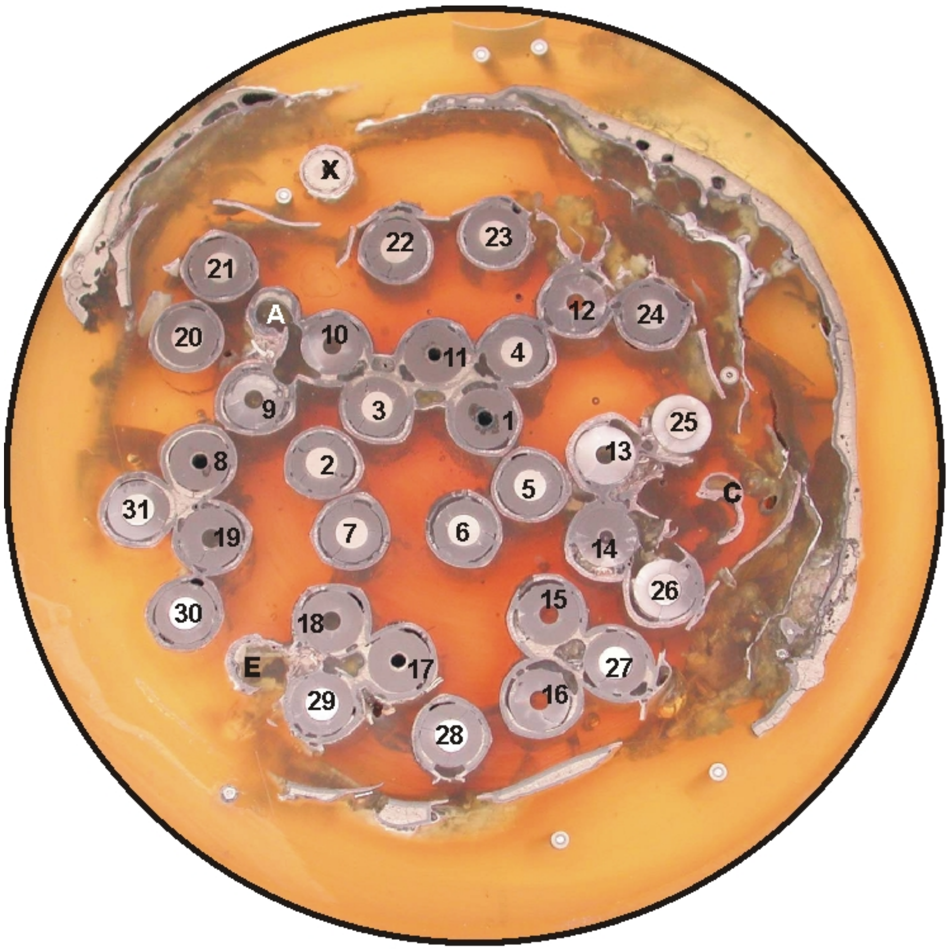

Elevation 950mm, top view

Elevation 934 mm, inverted to top view

QUENCH-12, level 950 mm; melt pool formation via necking mechanism

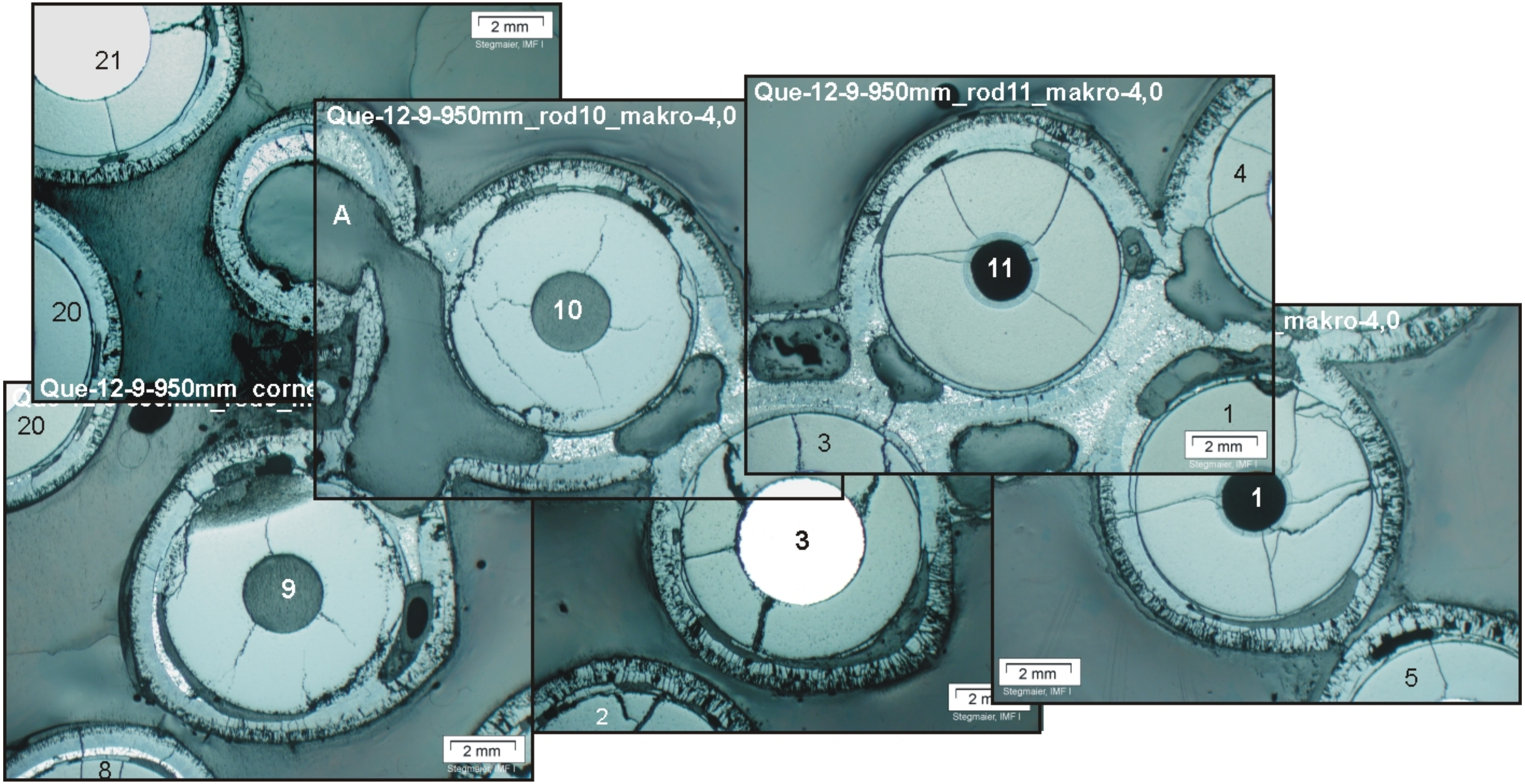

QUENCH-12, level 950 mm; dissolution of melt pool embedded cladding scale

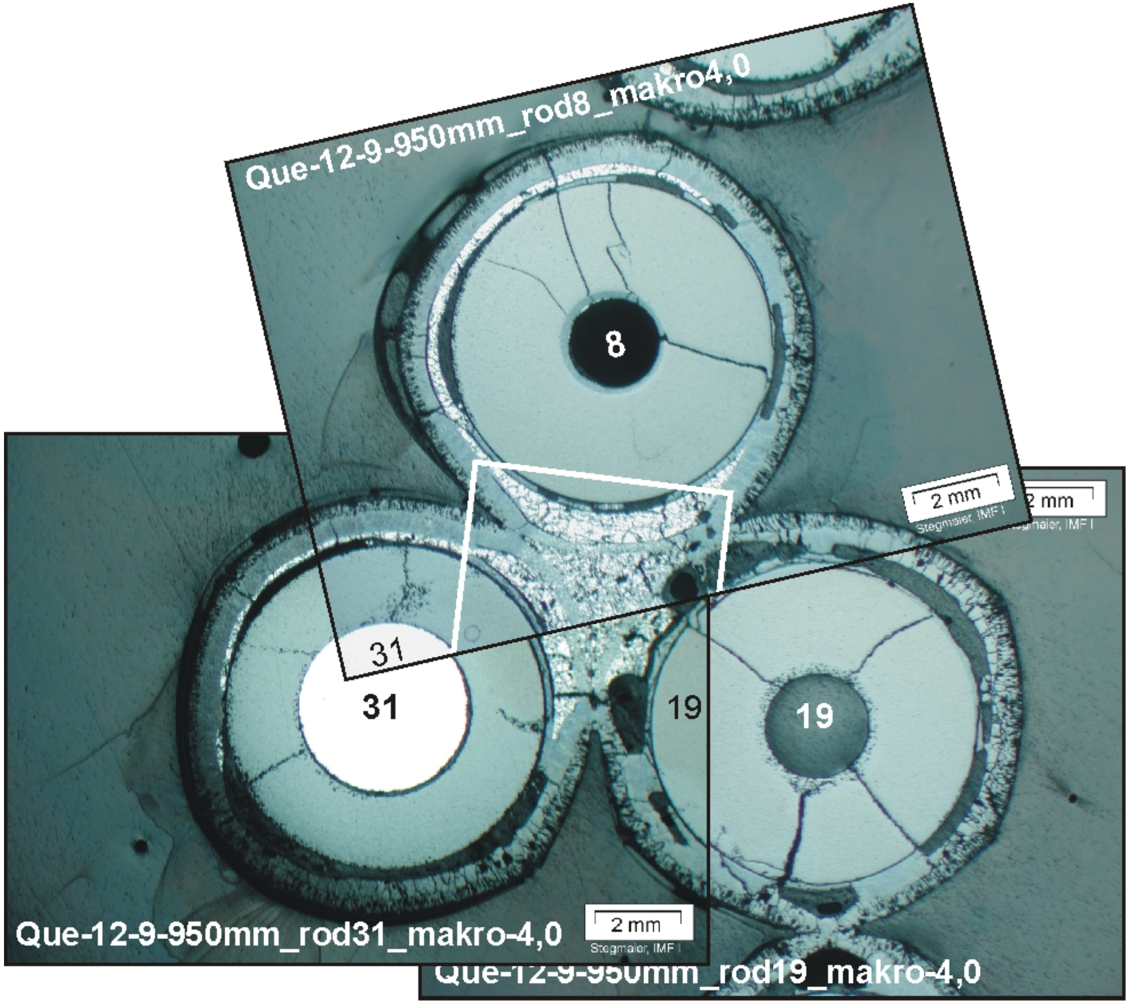

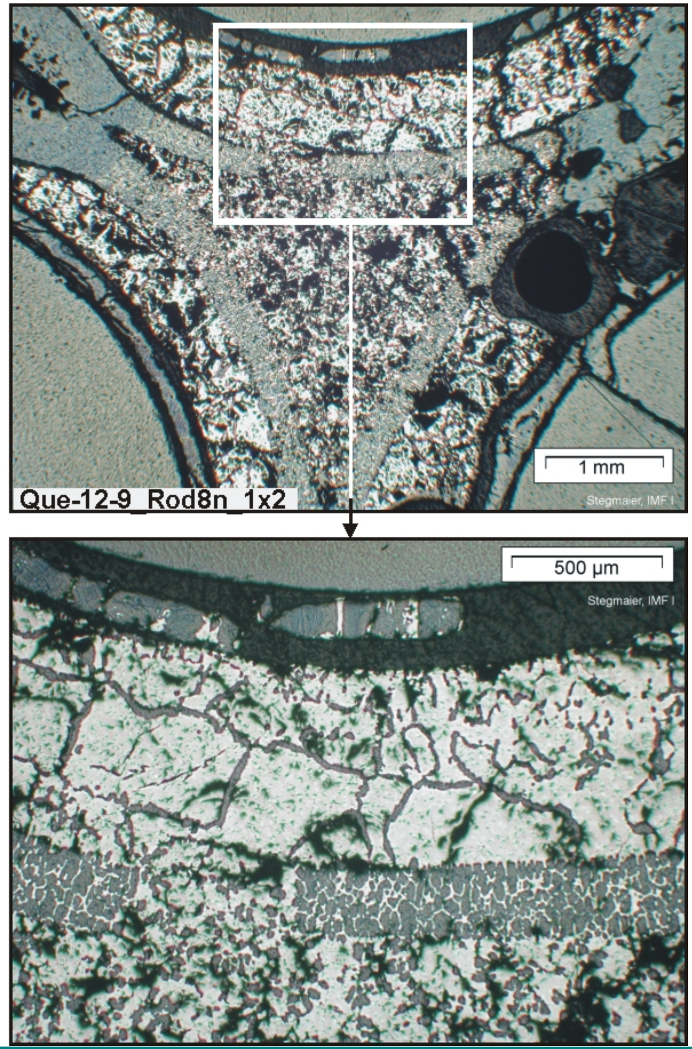

QUENCH-12, level 950 mm; oxidation items, seen after total cladding conversion

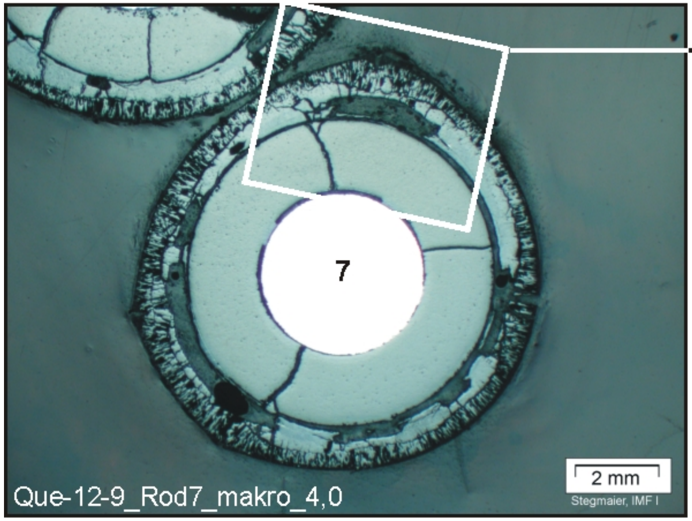

Notice:

Cracking and bulging of the external scale

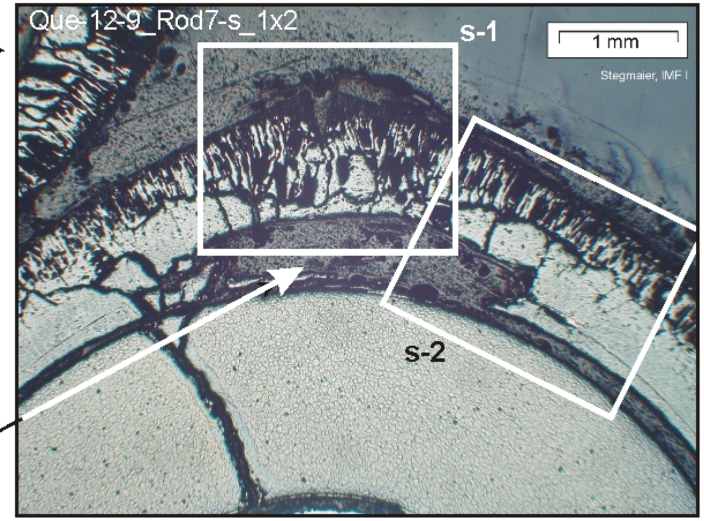

Void formed by melt relocation

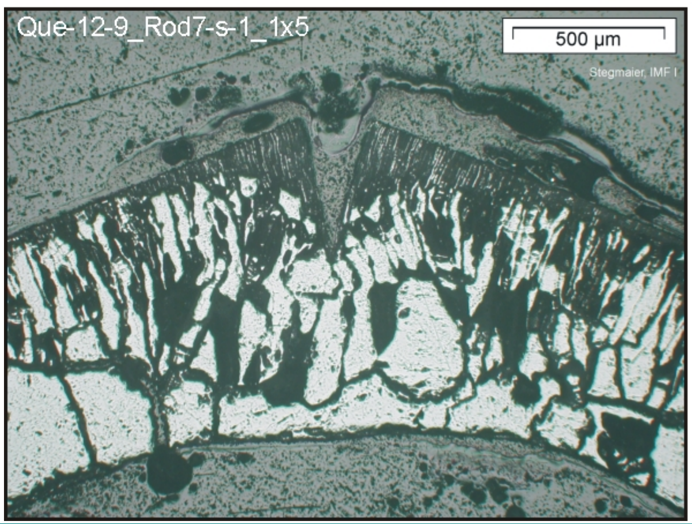

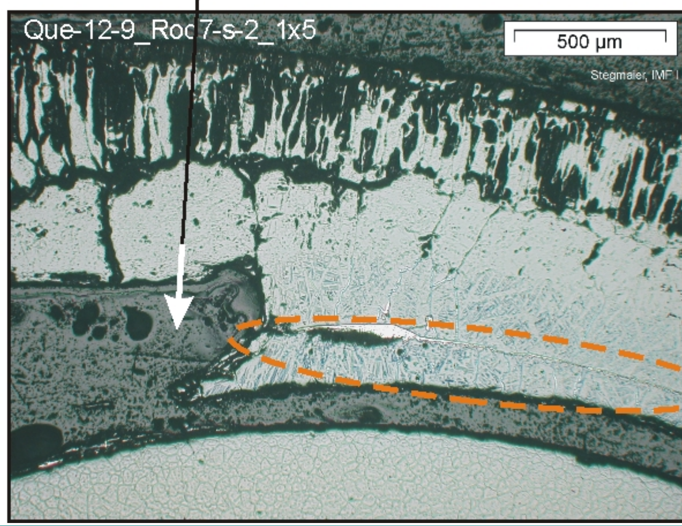

Oxidized pellet interaction layer

QUENCH-12, level 550 mm; oxidation of corner rod C

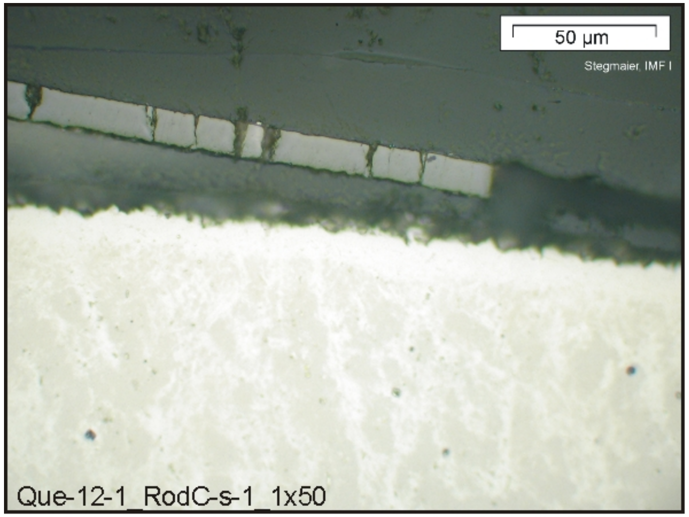

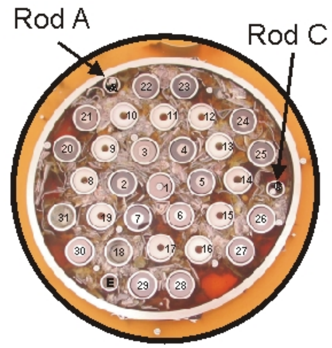

Que-12-01_550mm Rod C

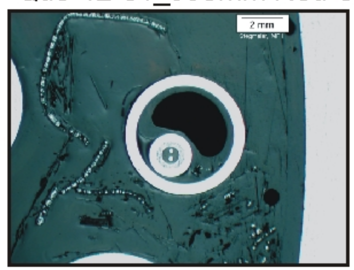

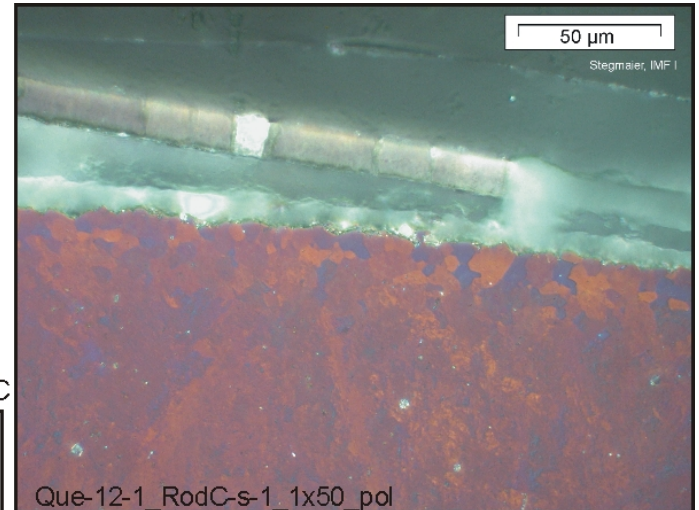

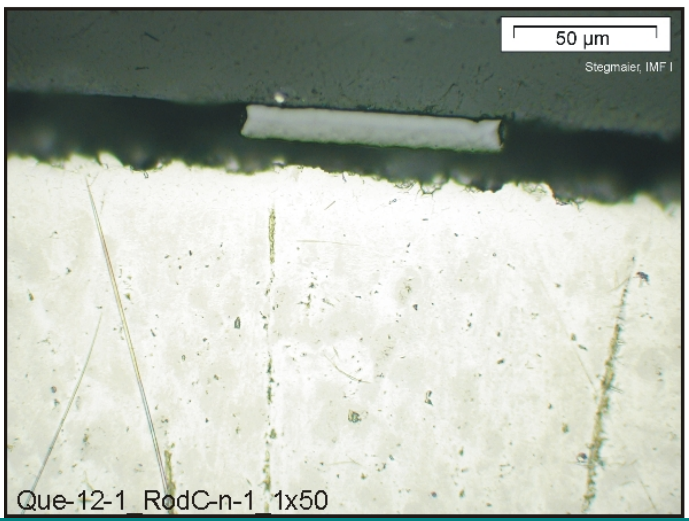

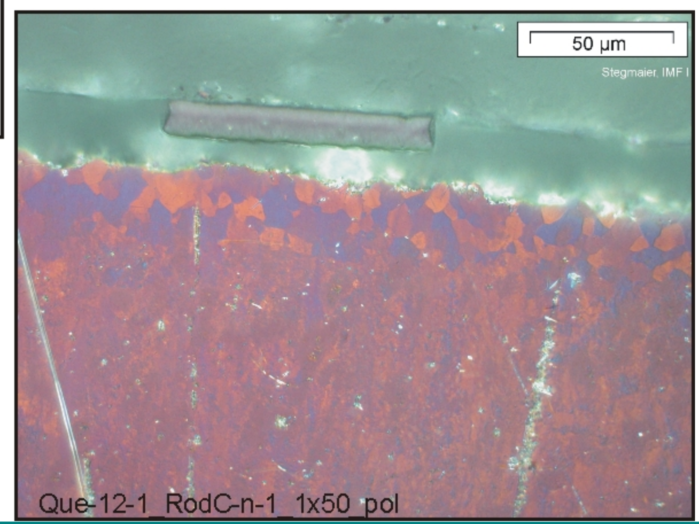

QUENCH-12, level 750 mm; oxidation of corner rods A (left) and C (right)

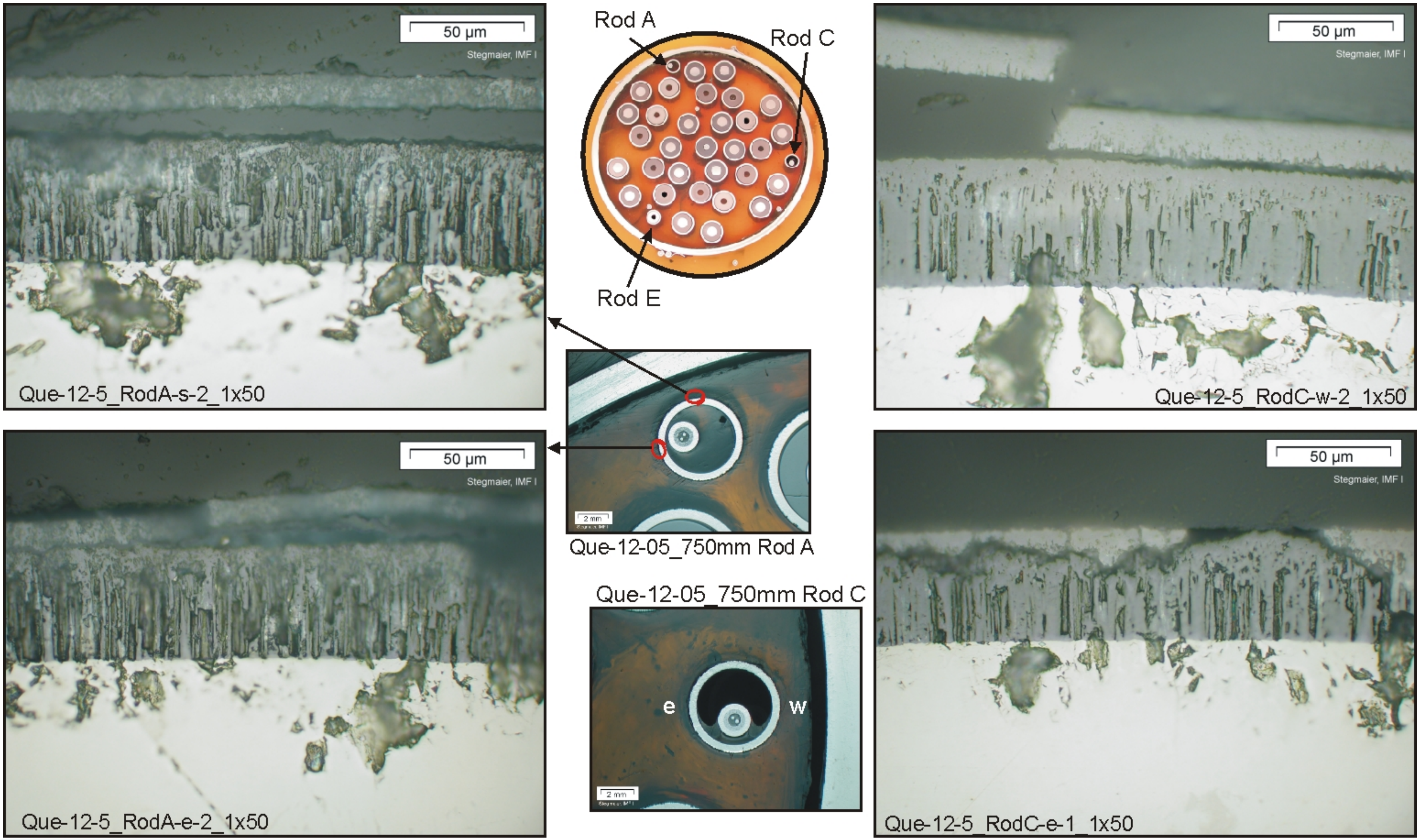

QUENCH-12, level 750 mm; oxidation of corner rod E

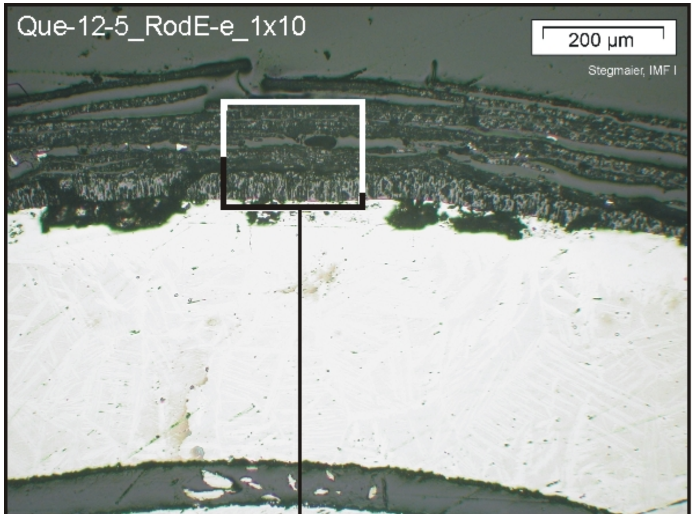

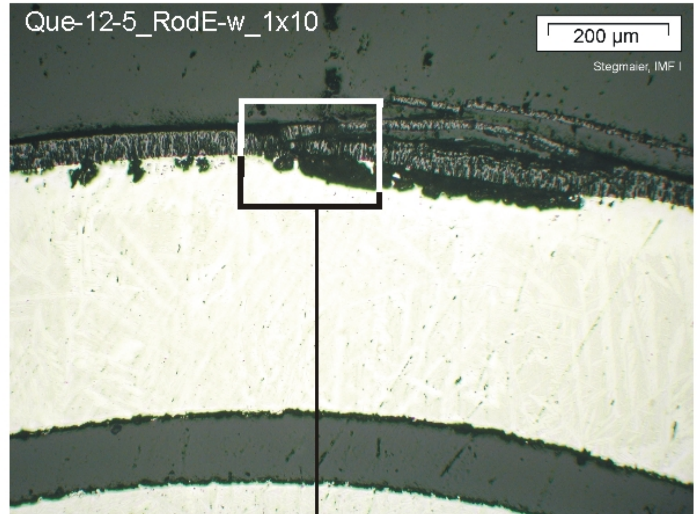

Orientation towards
east **west**

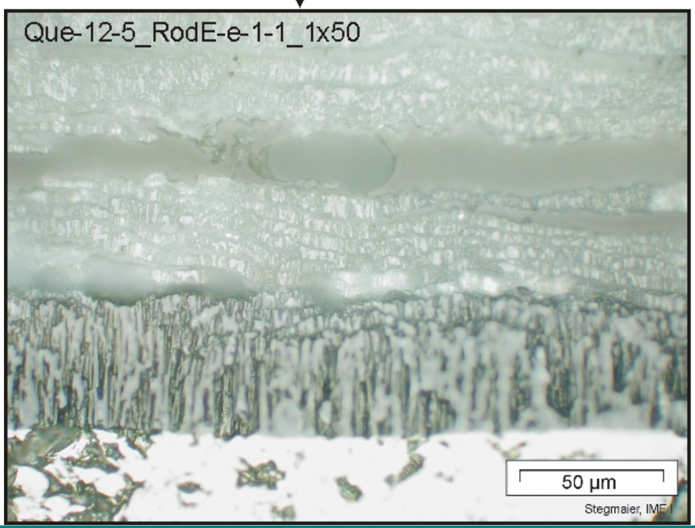

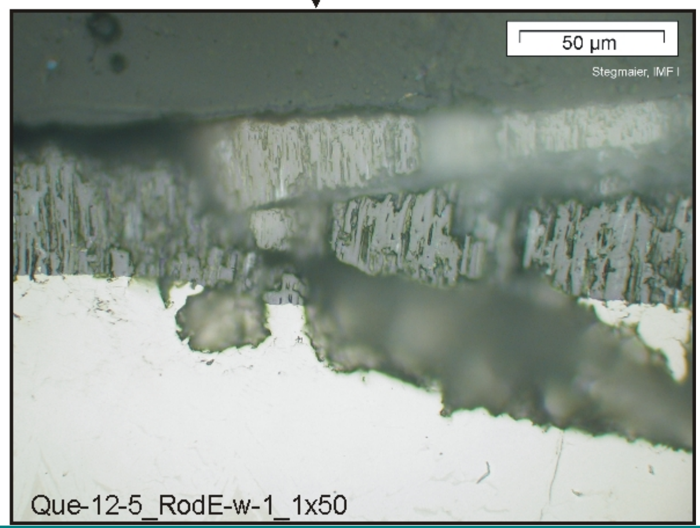

QUENCH-12, level 850 mm; oxidation of corner rods C (top) and E (bottom)

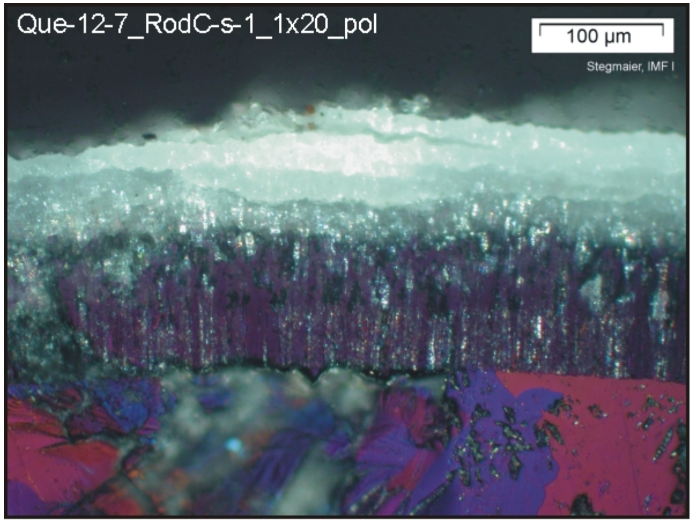

Que-12-07_850mm Rod C

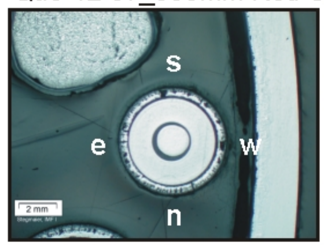

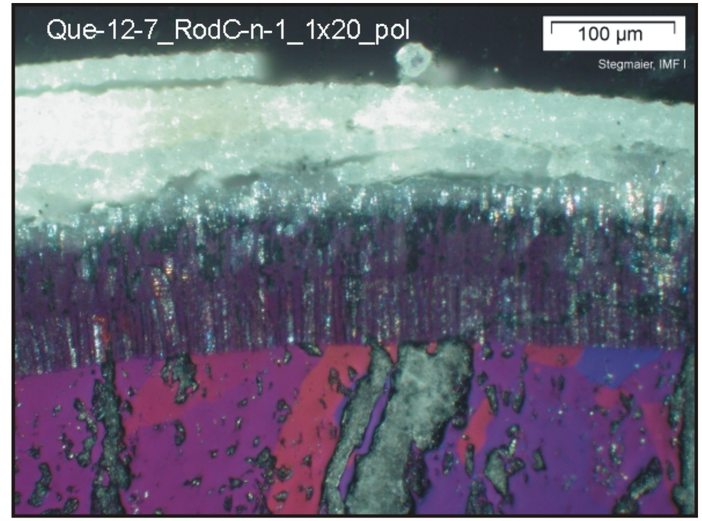

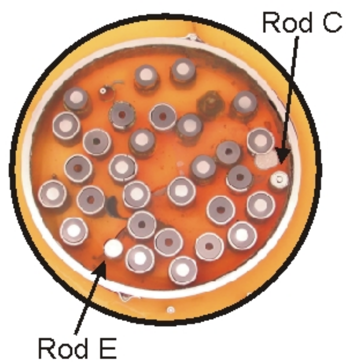

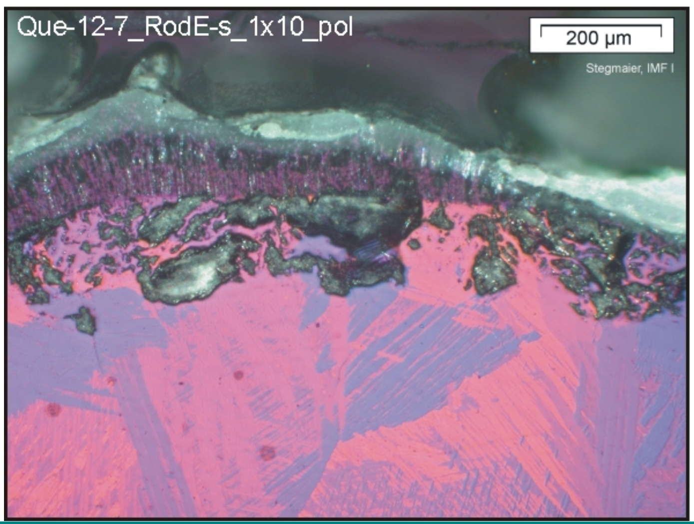

Que-12-07_850mm Rod E

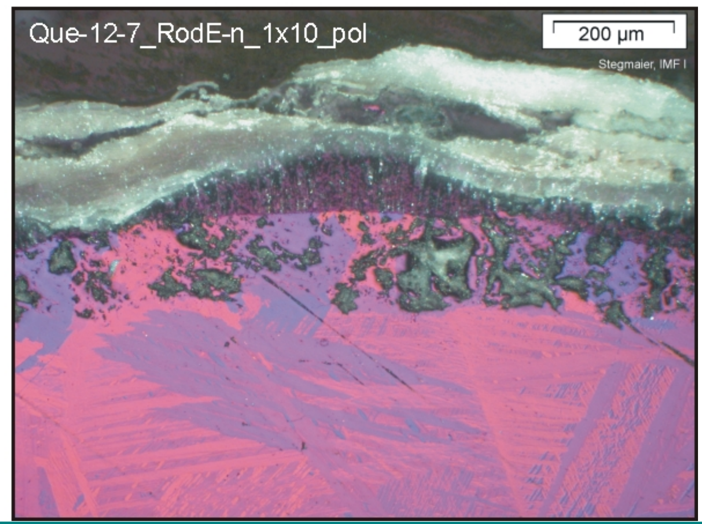

QUENCH-12, level 950 mm; oxidation of corner rod A

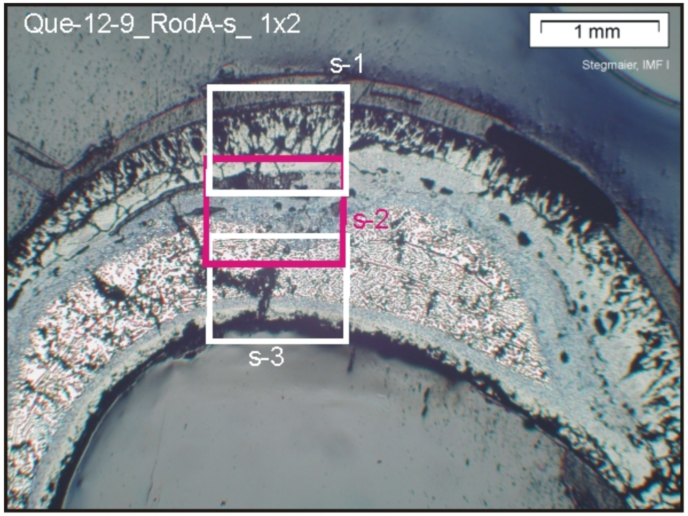

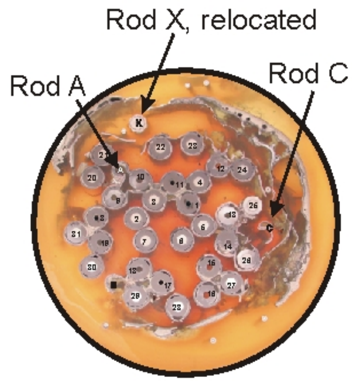

Que-12-09_950mm Rod A

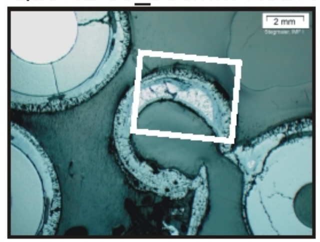

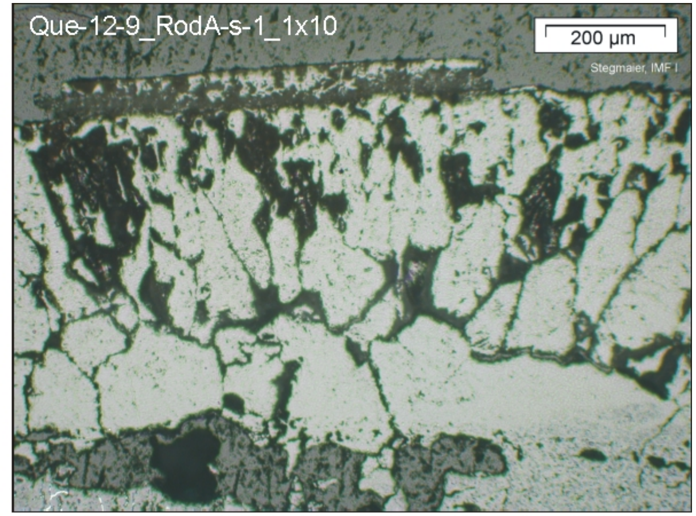

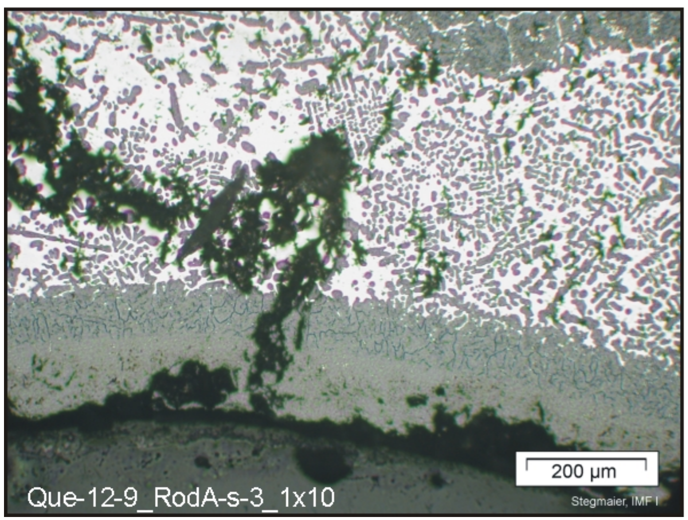

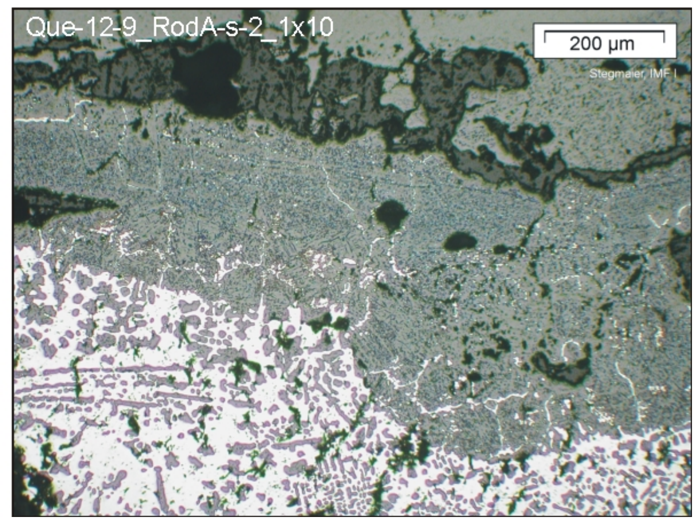

QUENCH-12; oxidation until quenching, according to withdrawn corner rod D at elevations 1120 mm (top) and 940 mm (bottom)

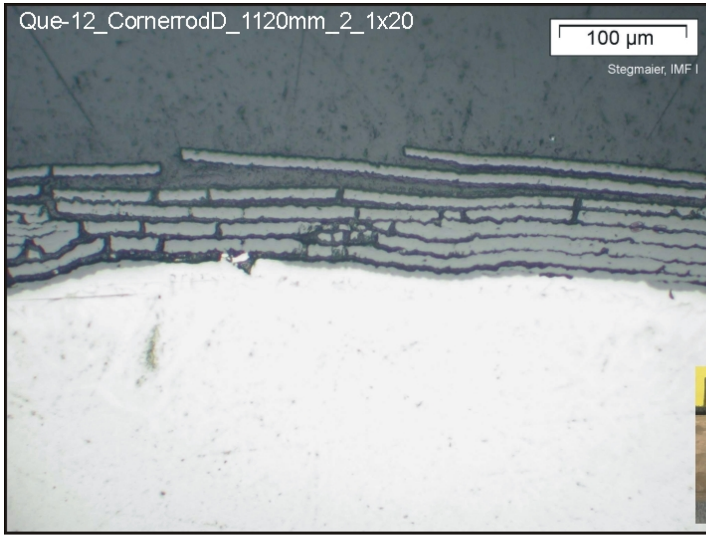

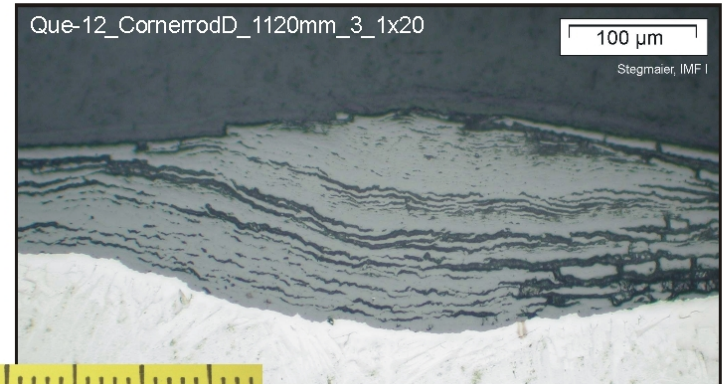

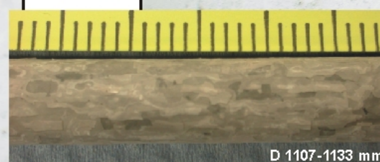

Side view of corner rod D around 1120 mm

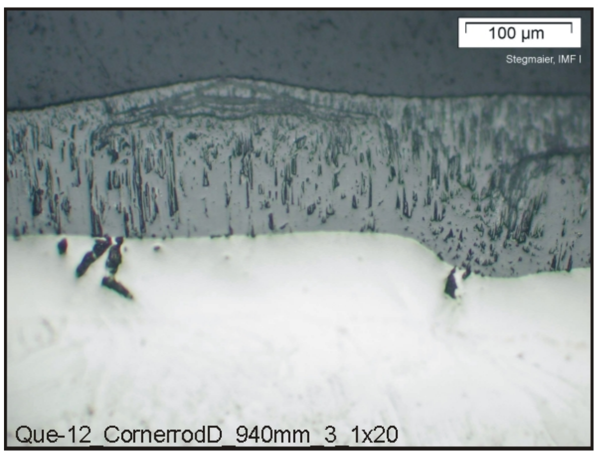

Side view of corner rod D around 940 mm

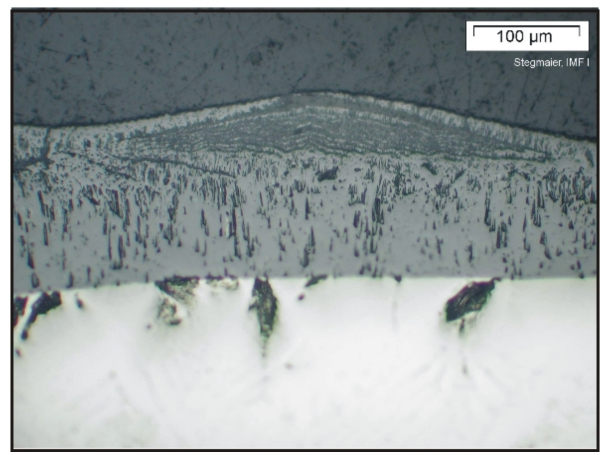

QUENCH-12, levels 550 and 650 mm; oxidation of the shroud (inner side)

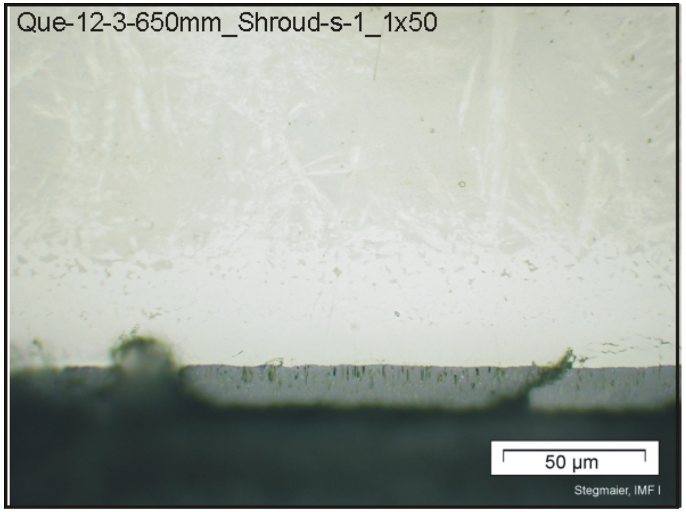

Elevation 650 mm

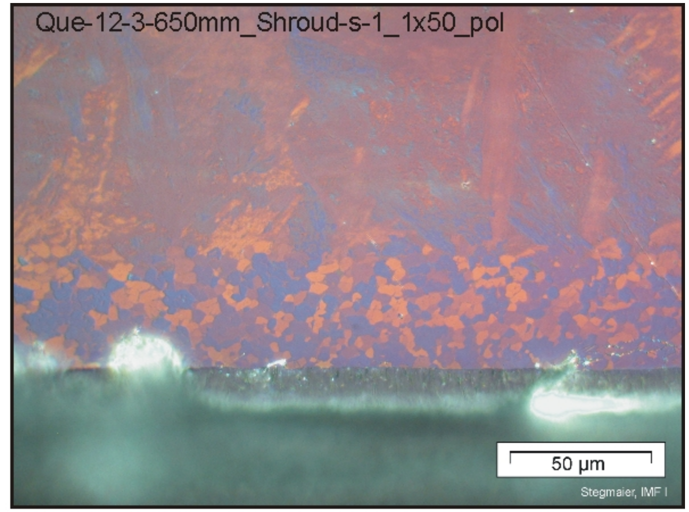

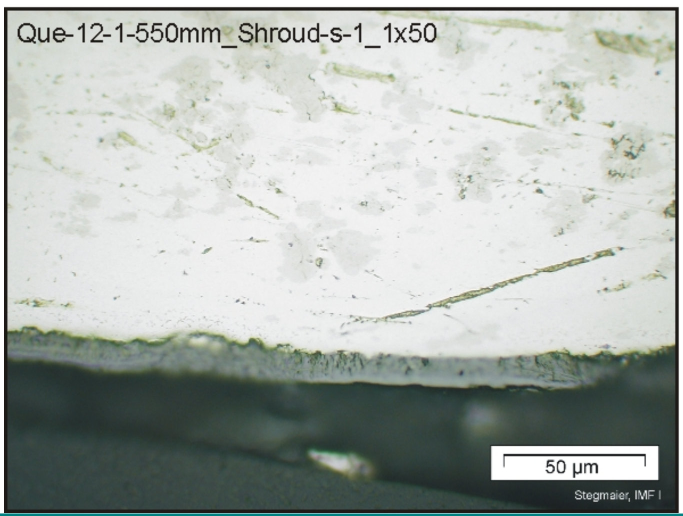

Elevation 550 mm

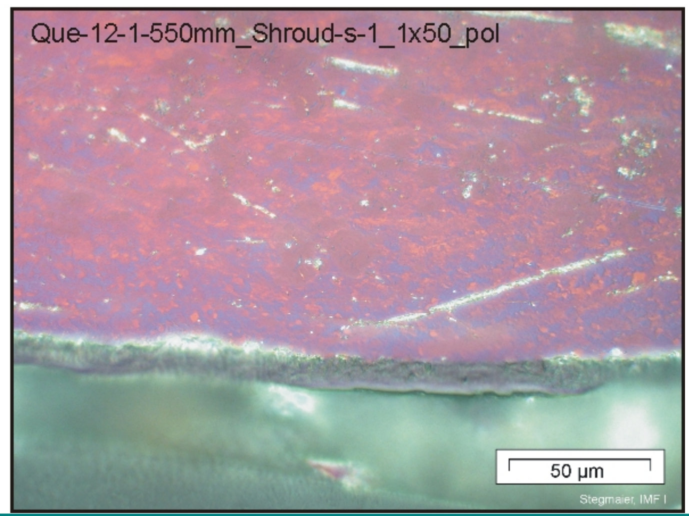

QUENCH-12, levels 750 and 850 mm; oxidation of the shroud (inner side)

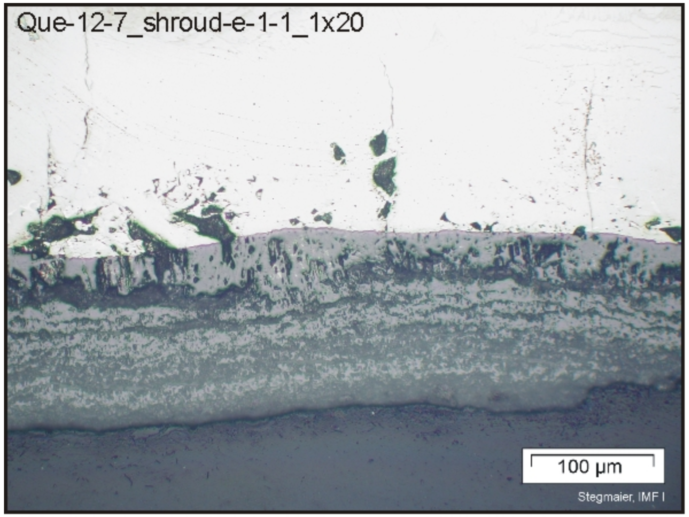

Level 850 mm

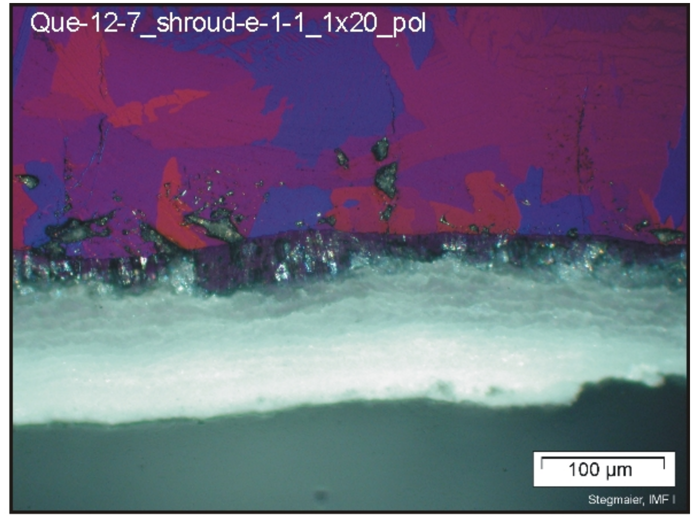

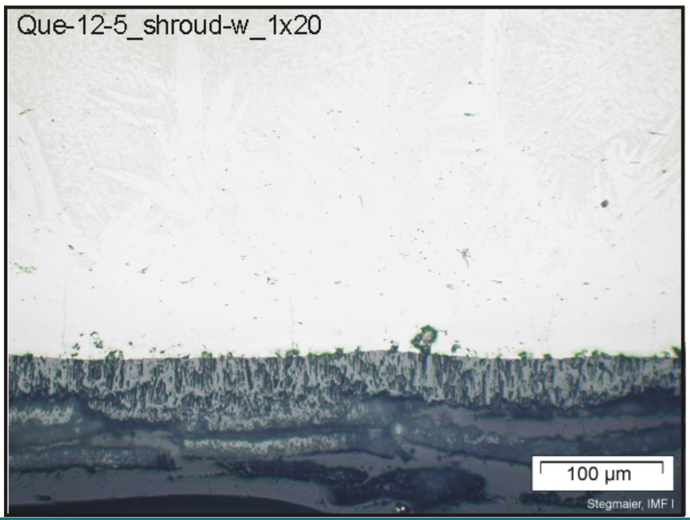

Level 750 mm

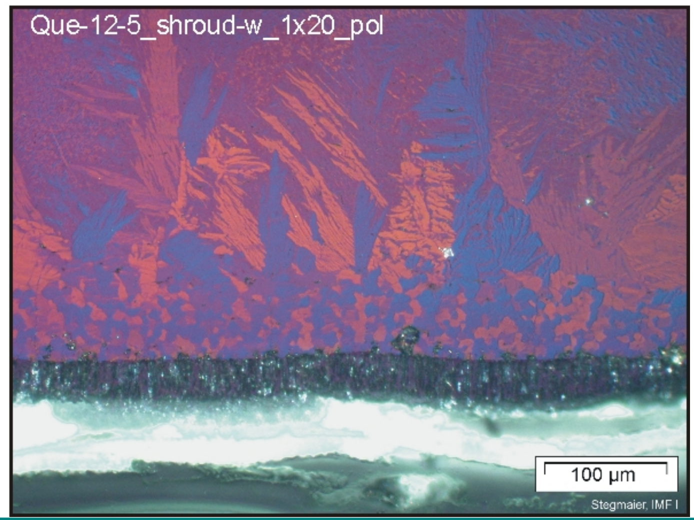

QUENCH-12, level 950 mm; oxidation of a shroud remnant towards south

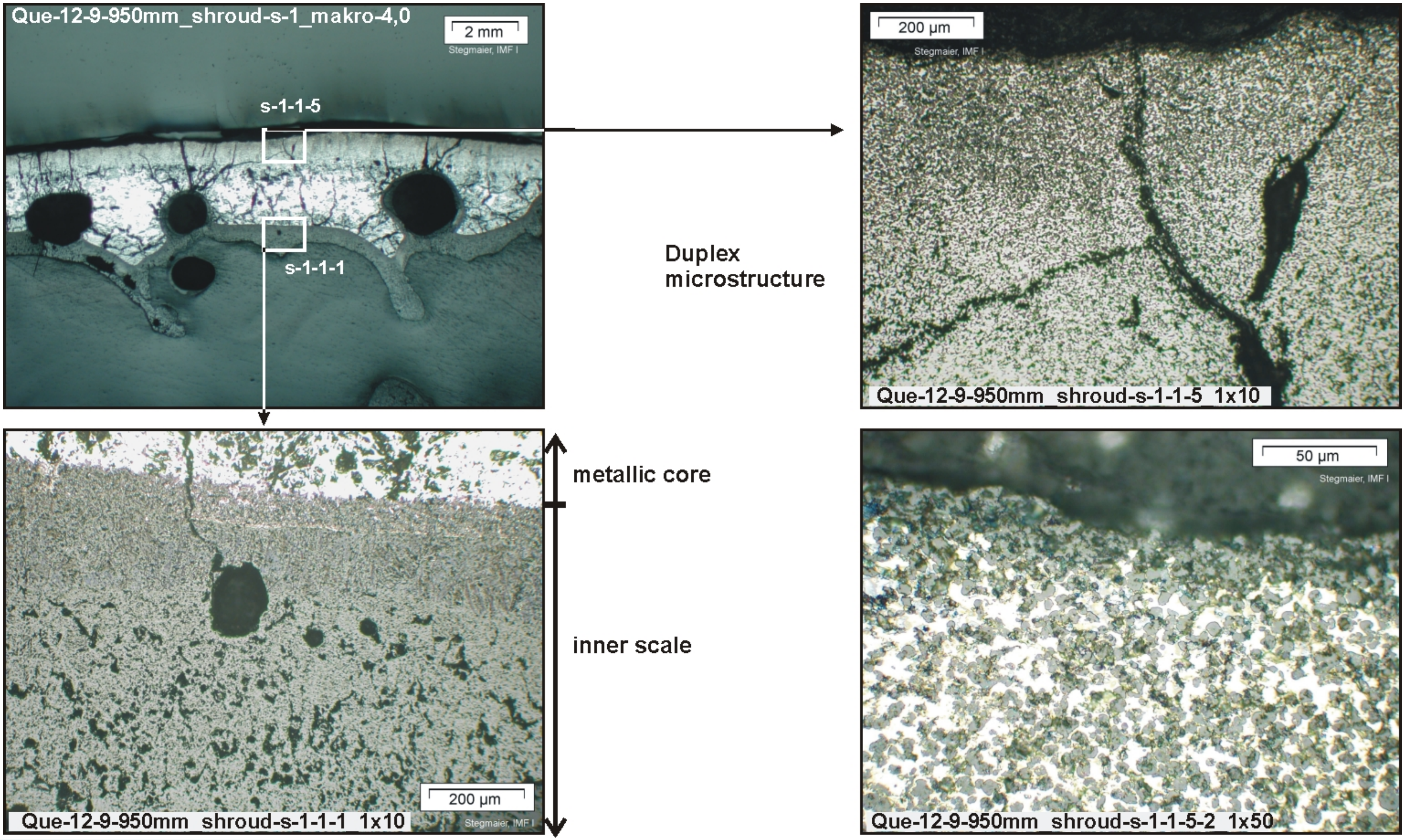

QUENCH-12; axial oxidation profiles, overview (left), details (right)

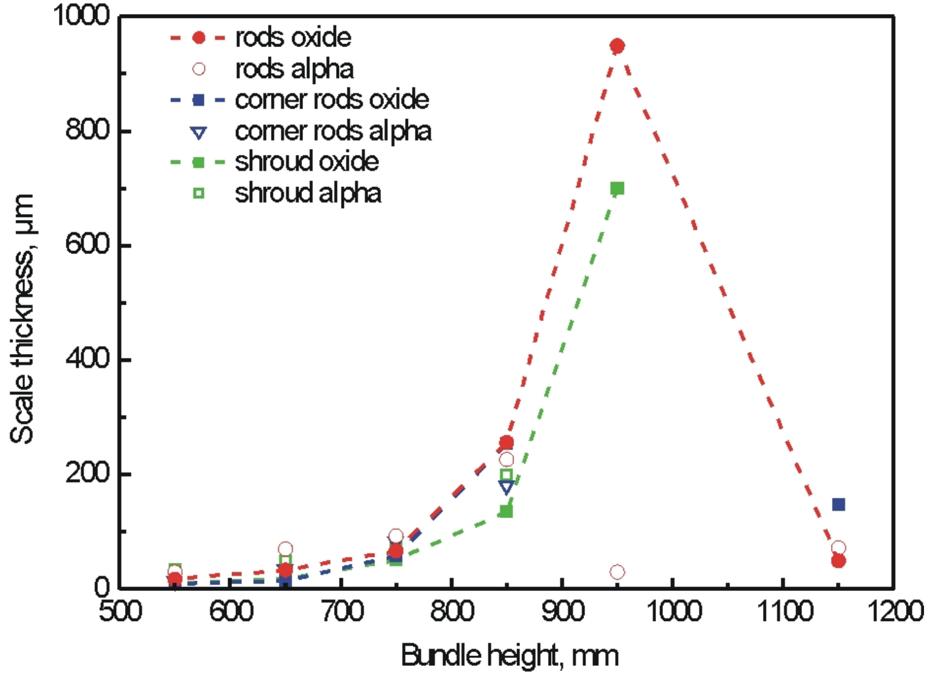

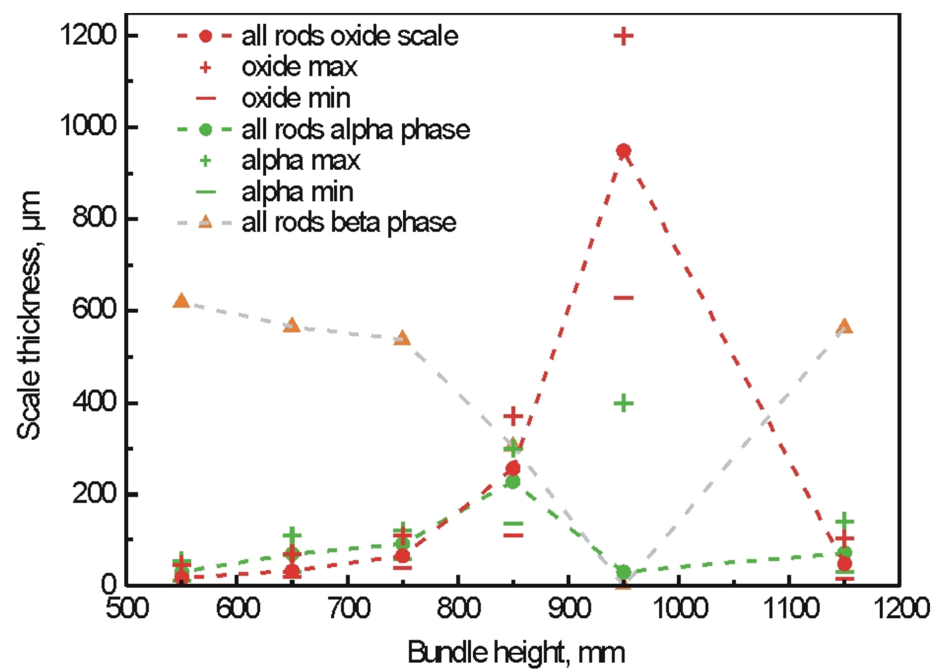

QUENCH-12, post-test analysis:
Axial distribution of the oxide layer on the surface of cladding tubes.
Measured residual oxide and oxide calculated on the base of residual metal

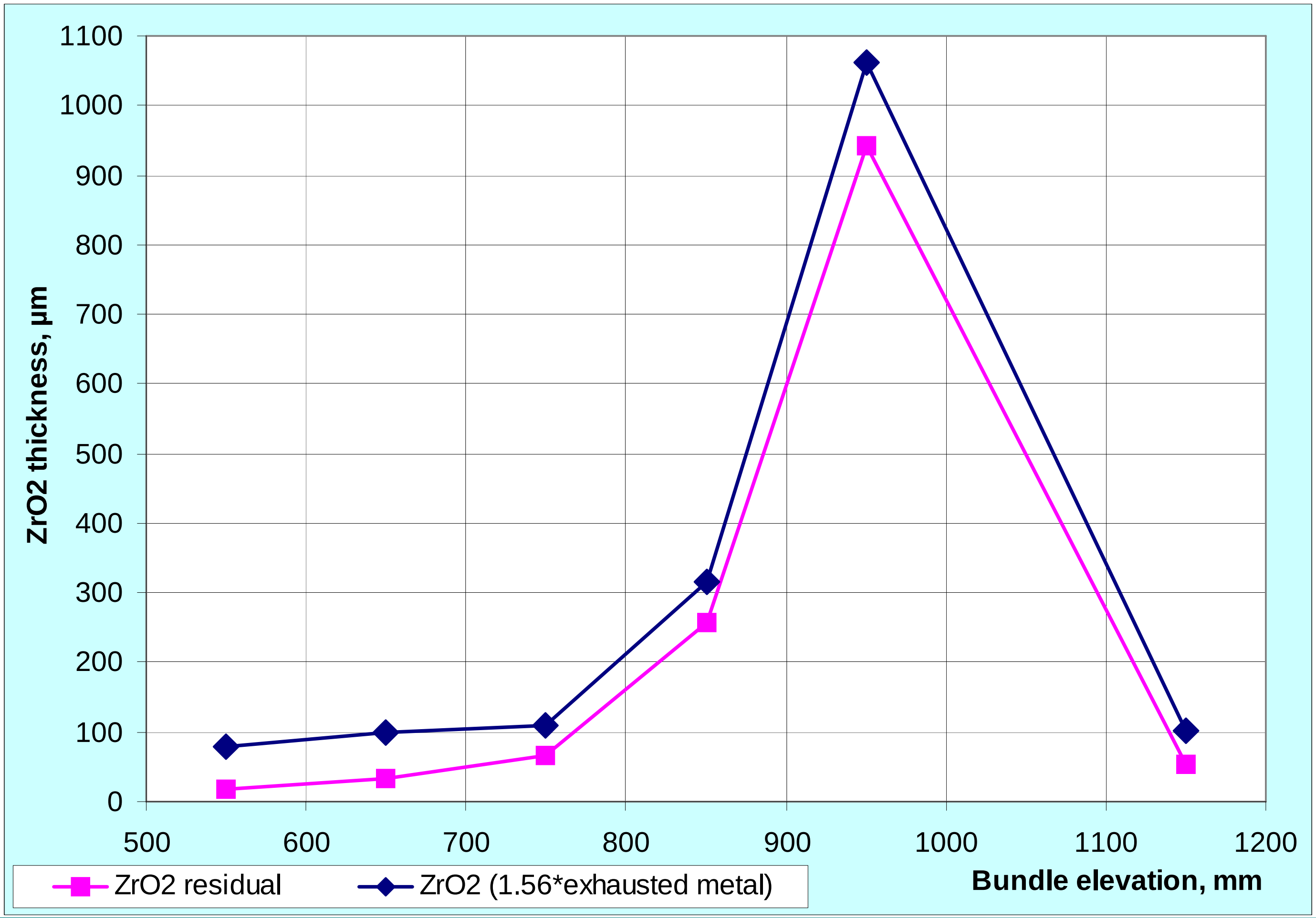

QUENCH-12: degree of oxide layer spalling for different bundle elevations

elevation	transient	*total oxide layer*	spalled oxide layer
1150 mm	1150...1650 K	*102 µm*	*54 µm* **(52%)**
950 mm	1350...2100 K	*1063 µm*	*123 µm* **(12%)**
850 mm	1300...1900 K	*316 µm*	*60 µm* **(19%)**
750 mm	1200..1600 K	*109 µm*	*43 µm* **(40%)**
650 mm	1150..1400 K	*100 µm*	*67 µm* **(67%)**
550 mm	1050..1200 K	*79 µm*	*62 µm* **(78%)**

Conclusive summary of QUENCH-12 PTE results

- During the pre-oxidation phase the Zr1%Nb (E110) cladding alloy is susceptible to breakaway oxidation within a certain temperature limit (up to ~1350 K for Zry-4). Oxide scale of layered type shows spalling into sub-layers and loss of fragments.
- Breakaway oxidation is found to continue into the transient phase depending on the elevation in the bundle. Determined by the temperature increase protective oxide with columnar growth type is formed below the defective top layer(s). This “recovery” beyond a breakaway regime limit is a remarkable and most safety relevant observation.
- The regular rod arrangement is retained up to ca. 800 mm. At next higher elevations rod-internal melting, melt re-distribution, and pellet/cladding chemical interaction have occurred.
- At the peak temperature level 950 mm the “necking” mechanism has resulted in melt pool formation, non-coherent melt relocation, dissolution of embedded scale, and melt oxidation.
- The breakaway typical oxidation in QUENCH-12 must be due to the Zr1%Nb cladding alloy since in QUENCH-06 the Zry-4 cladding was exposed to a very similar test conduct. The much higher hydrogen release during the reflood phase of QUENCH-12 can be the effect of the hydrogen evolution during the quench phase oxidation and a release of previously picked-up hydrogen. Both contributions may have been favored by the presence of post-transition scale with inferior barrier effect.